ELECTROWEAK INTERACTIONS OF HADRONS*

By J.-M. Gérard

Max-Planck-Institut für Physik und Astrophysik — Werner-Heisenberg-Institut für Physik, P.O. Box 40 12 12, Munich, West Germany

(Received November 7, 1989)

Constraints on physics beyond the standard model require a preliminary understanding of the interplay between the electroweak and strong interactions. Strong interaction effects are in principle non-negligible below the confining scale. A complementary approach, based on the meson-quark duality and applied on the $\pi^+ - \pi^0$ electromagnetic mass difference and the weak K-decays, confirms this expectation. Using this simple non-perturbative framework, we conclude that the $K_L - K_S$ mass difference, the empirical $\Delta I = \frac{1}{2}$ rule and the recently measured ε'/ε are consistent with the standard model.

PACS numbers: 12.10.Dm

Introduction

The standard model for strong and electroweak interactions [1] of quarks and leptons is based on the $SU(3)_C \times SU(2)_L \times U(1)$ gauge symmetries. The mediators of strong interactions, i.e. the gluons, as well as the quark matter fields are however not directly observable. Moreover, among the mediators of electroweak interactions, only the photon gives rise to long-range effects. These features, a priori unexpected for a so-called standard model, are explained by means of two crucial *assumptions*. On one hand, the asymptotically-free SU(3) gauge theory is confining at large distance such that only color-singlet hadron states appear in nature. On the other hand, the weak gauge sector is spontaneously broken via ad hoc self-interactions of fundamental scalar fields. But fundamental scalars immediately trigger the question of naturalness [2]. Why is the Fermi electroweak scale ($\Lambda_F \sim 10^2$ GeV) so small compared to the Planck scale ($\Lambda_P \sim 10^{19}$ GeV) at which new (gravitational) interactions become non-negligible? This question has been at the source of many interesting attempts to go beyond the standard model [3]. New symmetries (supersymmetry, ...) or new confining forces (technicolor, hypercolor) around the Fermi scale could cure this apparent sickness. Departures from the standard model, if any, should then show up around one TeV.

* Presented at the XXIX Cracow School of Theoretical Physics, Zakopane, Poland, June 2–12, 1989.

The other typical scale of the standard model is the strong interaction confining scale ($\Lambda_{QCD} \sim 1$ GeV). Below this scale, perturbation in terms of quarks and gluons stops being reliable and a formalism in terms of hadrons becomes obviously more appropriate.

It is well known that the physics of light bound-states and, in particular, of kaons has already been at the source of many important discoveries: parity violation, GIM mechanism (and the charm quark), *CP*-violation (and the top quark)... New high-precision measurements on light meson weak decays provide us with an indirect, but rather cheap, way to probe physics beyond the standard model, if any. However, *the more you try to know about physics above one TeV, the more you have then to understand physics below one GeV.* A typical example is the tiny $K_L - K_S$ mass difference. A better theoretical knowledge of the long distance, non-perturbative strong interaction contributions would allow us to put more stringent limits on possible $\Delta S = 2$ flavor changing neutral currents.

The purpose of these lectures is to present a new framework to treat effects of strong interactions on weak meson decays. In the first lecture (Section 1), we introduce the concept of chiral symmetry breaking which turns out to be the basic ingredient to build an appropriate strong interaction theory below the confining scale. A modified QCD theory and a linear σ model can effectively describe the breaking in terms of quark and meson fields, respectively.

In the second lecture (Sections 2, 3), we present the non-linear σ-model, a meson theory truncated to the pseudoscalars, which provides the Lagrangian for strong interactions at low momenta. This formalism allows not only a simple derivation of the "old" current algebra theorems but also an estimate of the size of chiral corrections. We then emphasize the role of the (axial)-vector mesons in the matching of the perturbative theory for strong interactions at low-momenta, i.e. the truncated non-linear σ-model, with the perturbative theory for strong interactions at high-momenta, i.e. QCD. A detailed illustration based on the $\pi^+ - \pi^0$ electromagnetic mass difference supports this complementary picture.

Finally, in the last lecture (Sections 4, 5, 6, 7), we adopt the same complementary picture for strong interactions to estimate the weak hadronic matrix elements associated with $K_L - K_S$ mass difference, the $\Delta I = \frac{1}{2}$ rule and with the *CP*-violating parameters ε and ε'. These are measured quantities which are rather sensitive to new physics beyond the standard electroweak model.

The aim of these lectures is certainly not to review the non perturbative methods available [4], but to plead in favour of the $\frac{1}{N}$ expansion approach [5] which provides a very simple link between the quark-gluon and meson theories for strong interactions. This approach is well-known as a qualitative way to describe strong interactions of light mesons [6]. As we will see, simple applications indicate that the $\frac{1}{N}$ expansion can be promoted at the rank of a quantitative tool for the study of the interplay of strong and electroweak interactions [7].

1. Strong interactions and chiral symmetry breaking

The SU(N) gauge-invariant QCD Lagrangian for quark degrees of freedom reads

$$\mathscr{L}_{\mathrm{QCD}}(q) = \bar{q}_{\mathrm{L(R)}}(i\not{D})q_{\mathrm{L(R)}} - [\bar{q}^a_{\mathrm{L}} m_{ab} q^b_{\mathrm{R}} + \mathrm{h.c.}], \tag{1.1}$$

with $q_{\mathrm{L,R}} \equiv \left(\frac{1 \mp \gamma_5}{2}\right) q$, the left (right)-handed projections of the quark field q and $a, b = 1 \ldots n$, the flavor indices. In Eq. (1.1) the summation over color indices is understood. In the limit where the quark (current) mass matrix m goes to zero, the QCD Lagrangian is also invariant under the global chiral $G_{\mathrm{f}} \equiv U(n)_{\mathrm{L}} \times U(n)_{\mathrm{R}}$:

$$q_{\mathrm{L,R}} \to g_{\mathrm{L,R}} q_{\mathrm{L,R}}; \quad g_{\mathrm{L,R}} \in U(n)_{\mathrm{L,R}}. \tag{1.2}$$

However, we know that the nucleon bound states, which transform nontrivially under G_{f}, are massive. Consequently, the chiral symmetry G_{f} must be broken below the one GeV confining scale. As we will see, this phenomenological input turns out to determine uniquely the low-momentum behaviour of strong interaction corrections to electroweak processes.

a) The Nambu and Jona-Lasinio model

A very interesting way to implement this chiral symmetry breaking is to add a non-renormalizable, but G_{f}-invariant, four-quark interaction [8].

$$\delta\mathscr{L}_{\mathrm{NJL}} \equiv \frac{G}{N} (\bar{q}^a_{\mathrm{L}} q^b_{\mathrm{R}}) (\bar{q}^b_{\mathrm{R}} q^a_{\mathrm{L}}) \tag{1.3}$$

to the QCD Lagrangian given in (1.1). The fermion bilinears are color singlets. The self-consistent (Dyson) equation to generate a dynamical "constituent" mass $\bar{m}$ (see Fig. 1)

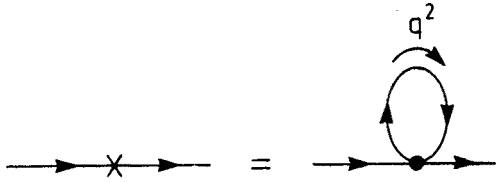

Fig. 1. The gap equation in the Nambu and Jona-Lasinio model. The cross denotes a dynamical quark mass and the dot stands for the four-quark coupling defined in Eq. (1.3)

gives the following relation:

$$\bar{m}_a = 2G \frac{i}{(2\pi)^4} \int \frac{\bar{m}_a}{q^2 - \bar{m}_a^2} d^4_q + O\left(\frac{1}{N}\right) \tag{1.4}$$

if one neglects the quark current masses. The factor two in Eq. (1.4) arises from the two possible contractions of the quark fields in Eq. (1.3). For reasons which will become mani-

fest later, we neglect the color-suppressed contribution. Eq. (1.4) is trivially satisfied if $\bar{m}_a \equiv 0$. However, if the effective coupling G is large enough, namely

$$G > G_{\text{critical}} \equiv \frac{8\pi^2}{M^2}, \tag{1.5}$$

Eq. (1.4) also allows the non-perturbative solution

$$\frac{\bar{m}_a^2}{M^2} \log\left(1 + \frac{M^2}{\bar{m}_a^2}\right) = 1 - \frac{8\pi^2}{GM^2}. \tag{1.6}$$

The Euclidean ultraviolet cut-off introduced in Eq. (1.4) is expected to be around the confining scale. We assume $M = 1$ GeV to plot the graph of Eq. (1.6) in Fig. 2. The equation

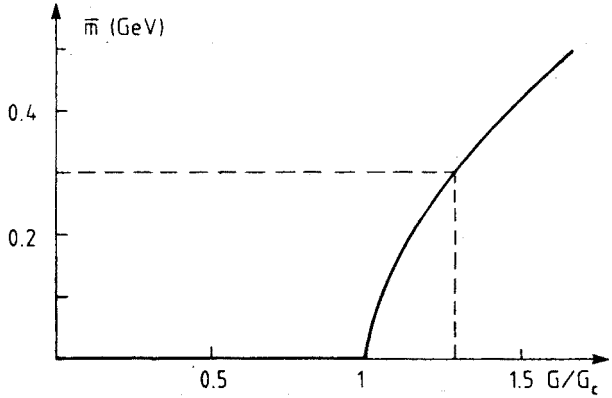

Fig. 2. The dynamical quark mass as a function of the effective coupling G defined in Eq. (1.3)

of motion derived from the Lagrangian given in (1.1) and (1.3) implies a relation between the "constituent" mass $\bar{m}$ and the quark-antiquark condensate:

$$\bar{m} = -\frac{G}{2N}\langle 0|\bar{q}q|0\rangle \tag{1.7}$$

if one neglects again the quark "current" masses. The $\bar{q}q$ condensate plays therefore the role of an order parameter. If $\langle\bar{q}q\rangle = 0$, the chiral symmetry G_f remains unbroken and massless nucleons appear in parity doublets. On the other hand, if $\langle\bar{q}q\rangle \neq 0$, G_f is broken and the nucleons are massive. For $\bar{m} = 300$ MeV $\simeq \frac{m_{\text{nucleon}}}{3}$, we obtain (see Fig. 2)

$$\langle\bar{q}q\rangle \simeq -(0.26\ \text{GeV})^3 \tag{1.8}$$

in fair agreement with QCD sum rules [9].

The analogy with the theory of superconductivity [10] is quite striking and it is therefore natural to investigate the possibility of deriving a Ginzburg-Landau type of effective Lagrangian for the $(\bar{q}q)$ order parameter. At low temperature, the attractive interaction mediated

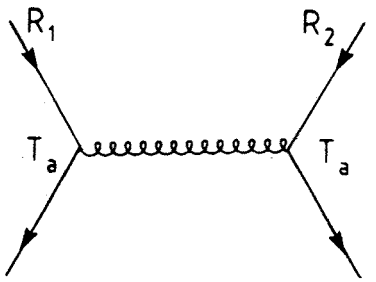

Fig. 3. Single gluon exchange interaction between colored fermions transforming like the irreducible representation R_i of $SU(N)_c$

by phonon exchange between two electrons with opposite spin and momenta leads to the formation of "Cooper pairs". Similarly, at low-momentum, the strong coupling α_s becomes in principle large enough to produce bound states of colored fermions (see Fig. 3). In the one-gluon approximation, the effective static potential reads [11]

$$V = \alpha_s T_a(R_1) T_a(R_2)$$

$$\equiv \frac{\alpha_s}{2} \{C_2(R \supset R_1 \otimes R_2) - C_2(R_1) - C_2(R_2)\}, \tag{1.9}$$

where R_i and R are the $SU(N)_c$ representations of the colored fermion i and of the bound state, respectively. The quadratic Casimir $C_2(R)$ for the lowest representations of $SU(N)_c$ are given in Table I.

TABLE I

dim (R)	$C_2(R)$
1	0
N	$\frac{N^2-1}{N}$
$\frac{N(N+1)}{2}$	$\frac{2(N-1)(N+2)}{N}$
$\frac{N(N-1)}{2}$	$\frac{2(N+1)(N-2)}{N}$
N^2-1	$2N$

It is then straightforward to realize that only the color-singlet channel of the $q\bar{q}$ interaction and the antisymmetric channel of the qq interaction are attractive:

$$V = -\left(\frac{N^2-1}{N}\right)\alpha_s \quad \text{for} \quad (q\bar{q})_1,$$

$$V = -\left(\frac{N+1}{N}\right)\alpha_s \quad \text{for} \quad (qq)_{AS}. \tag{1.10}$$

However, the single-gluon approximation used here is far from being convincing since α_s at one GeV is of order one. A non-perturbative treatment is necessary.

The $\frac{1}{N}$ expansion approach [5] in $SU(N)_{QCD}$ turns out to be rather suitable for problems involving bound states. Furthermore, this approach provides us with a simple diagrammatic link between the usual quark-gluon and the meson pictures for strong interactions.

b) The diagrammatic rules of $\frac{1}{N}$ expansion

The Feynman diagram approach to $\frac{1}{N}$ expansion is based on two extremely simple rules [5, 6]. First, a quark field q^i carries the color index i with $i = 1 \ldots N$. Consequently, any quark-loop is proportional to the number of colors N (see Fig. 4a). On the other

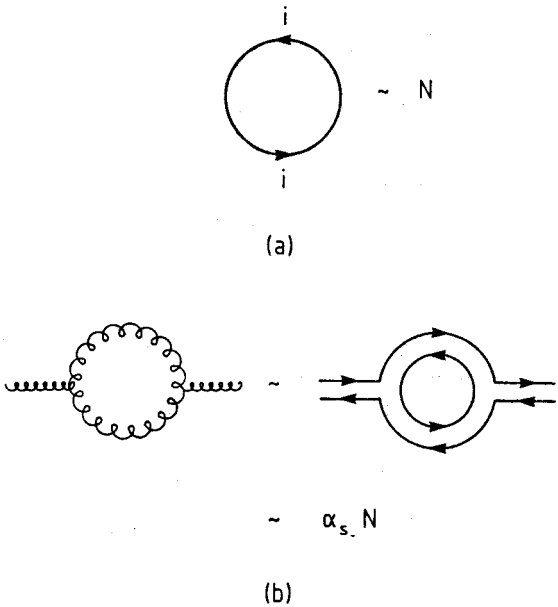

Fig. 4. The diagrammatic rules of $\frac{1}{N}$ expansion. The full line is a quark, the curly line denotes a gluon

hand, a gluon field $G^i_{\mu j}$ carries two color indices and can be symbolically represented by a $q^i\bar{q}_j$ quark pair. From the behaviour of the vacuum polarization diagram in the large-N limit (see Fig. 4b), we can immediately infer that

$$\alpha_s \sim \frac{1}{N} \tag{1.11}$$

in order to maintain $SU(N)_c$ — QCD nontrivial.

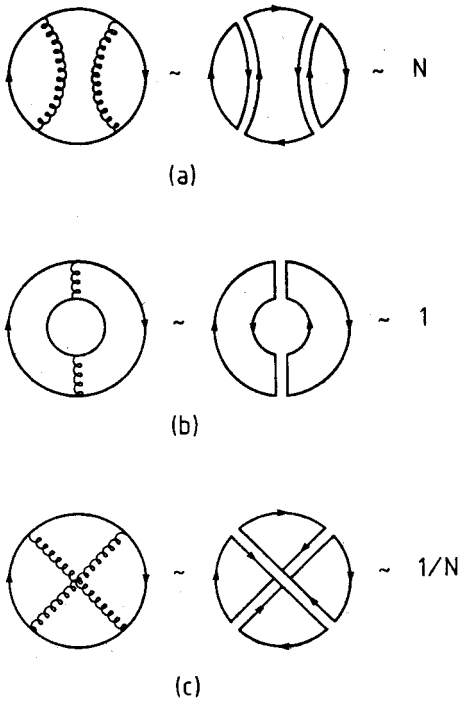

Fig. 5. Selection rules of the $\frac{1}{N}$ expansion

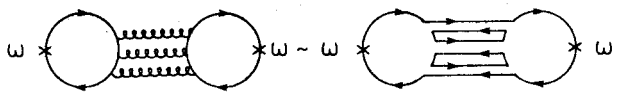

Fig. 6. The next-to-leading contribution to the isospin-singlet ω-vector-meson

These rules imply then two selection rules which are left as an exercise (see Fig. 5):

(*i*) "internal quark-loop effects are suppressed by $\frac{1}{N}$" (Fig. 5b);

(*ii*) "non-planar diagrams are suppressed by $\frac{1}{N^2}$" (Fig. 5c).

It is well-known that the large-N approximation provides us with a good qualitative picture of strong interactions at low q^2, where the α_s perturbative expansion is not valid anymore. After all, the empirical Zweig rule for the light vector mesons can only be understood in the framework of the $\frac{1}{N}$ expansion. For example, isospin implies that the next-to-leading three-gluon exchange diagram (see Fig. 6) contributes to the ω (783) but not to the ϱ (770) vector meson masses. The observed degeneracy in mass indicates that the large-N approximation makes indeed sense at a scale where perturbative QCD is no more reliable.

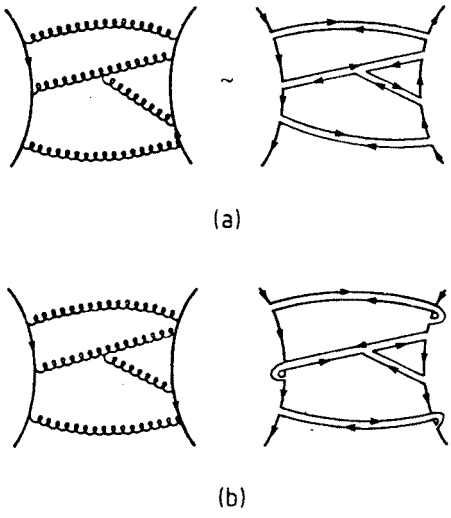

Fig. 7. (a) Planar $q\bar{q}$ and (b) non-planar qq strong interactions

Let us therefore consider the large-N limit in Eq. (1.10). Using Eq. (1.11), we conclude that in this limit, only the $q\bar{q}$ color singlet channel is attractive. Moreover, the non-perturbative nature of the $\frac{1}{N}$ expansion provides now a way to go beyond the single gluon approximation. The sum over the leading planar diagrams with an arbitrary number of gluons (Fig. 7a) implies that only the $q\bar{q}$ color singlet channel remains attractive in the large-N limit, the qq interaction being non-planar (Fig. 7b). Let us then introduce the local order parameter

$$\chi_a^b \equiv q_L^b \bar{q}_a^R \tag{1.12}$$

which transforms (see Eq. (1.2)) like

$$\chi \to g_L \chi g_R^+ \tag{1.13}$$

under the chiral symmetry $G_f \equiv U(n)_L \times U(n)_R$. The most general G_f-invariant effective potential for χ is given by

$$\mathscr{L} G_f = N \operatorname{Tr} F(\chi\chi^+) + [\operatorname{Tr} G(\chi\chi^+)]^2 + \dots , \tag{1.14}$$

where the dots stand for terms with more than two flavor traces. The first term in Eq. (1.14) arises from the (infinite) sum over the leading planar quark "bubbles" (one flavor trace). The second one is induced by bubbles with one internal quark loop (two flavor traces) and is therefore $\frac{1}{N}$ suppressed (see Fig. 5b). In the large-N approximation, only the single flavor trace term of Eq. (1.14) survives and the vacuum expectation value of $\chi\chi^+$ is necessarily proportional to the identity [12]. The chiral group G_f is either spontaneously broken into its diagonal vector subgroup $U(n)_{L+R}$ or remains unbroken. For $n \geqslant 3$, the latter

possibility is simply ruled out by the nice 't Hooft anomaly matching conditions [2]. We conclude that in a world with three light flavors ($m_{u,d,s} \ll 1$ GeV), we have the following breaking pattern:

$$U(3)_L \times U(3)_R \to U(3)_{L+R}$$

in the large-N approximation [12].

We emphasize again the real power of the $\frac{1}{N}$ expansion which provides a simple diagrammatic link between the quark-gluon and the meson pictures. We have seen that the large-N limit is consistent with two important features of the strong interactions, namely confinement and chiral symmetry breaking. Let us then consider the simplest effective theory satisfying these properties.

c) The linear σ-model

In the large-N limit, the most general dimension-four chiral-invariant Lagrangian for the χ-scalar field reads

$$\mathscr{L}_L = \tfrac{1}{2} \operatorname{Tr} \partial_\mu \chi \partial^\mu \chi^+ - c \operatorname{Tr}\left(\chi\chi^+ - \frac{f^2}{4}\right)^2 \tag{1.15}$$

with $c > 0$. The complex order parameter χ can be expressed in terms of a nonet of scalars σ and a nonet of pseudoscalars π:

$$\chi \equiv \frac{1}{\sqrt{2}}(\sigma + i\pi); \quad \sigma = \sigma_\alpha \lambda^\alpha, \quad \pi = \pi_\alpha \lambda^\alpha, \tag{1.16}$$

where λ_α ($\alpha = 0, \ldots 8$) are the usual three-by-three Gell-Mann matrices. The chiral symmetry breaking is triggered by the non-vanishing vacuum expectation of σ. Assuming $\langle \sigma_3 \rangle = 0$ (isospin approximation), we find two degenerate minima:

$$\langle \chi \rangle = \begin{pmatrix} 1 & & \\ & 1 & \\ & & \pm 1 \end{pmatrix} \frac{f}{2}. \tag{1.17}$$

The chimeral solution with a negative sign gives rise to four kaon-like scalar Goldstone bosons (see Eq. (1.23)). Let us therefore consider the more realistic minimum:

$$\langle \sigma_8 \rangle = 0, \quad \langle \sigma_0 \rangle = \frac{\sqrt{3}}{2} f. \tag{1.18}$$

The mass spectrum is then the following:

$$m_\sigma = \sqrt{\frac{8c}{3}} \langle \sigma_0 \rangle, \quad m_\pi = 0 \tag{1.19}$$

namely a degenerate nonet of massive scalars and nine pseudoscalar Goldstone bosons associated with the spontaneous breaking of the flavor symmetry G_f. Explicit breaking terms are therefore required to reproduce the observed mass spectrum of the "light" π, K, η and η' pseudoscalars [13]

$$\mathscr{L}_{\text{breaking}} = \frac{f_r}{4} \operatorname{Tr} m(\chi+\chi^+) + \frac{\alpha f^2}{32N} [\log\det\chi - \log\det\chi^+]^2. \tag{1.20}$$

The first term breaks the G_f symmetry, while the second one breaks only its axial U(1) subgroup and gives the η' a larger mass (see Section 2). In Eq. (1.20), m denotes the diagonal quark current mass matrix:

$$m = \begin{pmatrix} m_u & & \\ & m_d & \\ & & m_s \end{pmatrix}. \tag{1.21}$$

In the isospin limit we have $m_u = m_d \neq m_s$ and the flavor SU(3) breaking is triggered by the non-vanishing expectation value of the σ_8 component:

$$\Delta \equiv -\frac{\langle\sigma_8\rangle}{\langle\sigma_0\rangle} \neq 0. \tag{1.22}$$

The parameter Δ introduced in Eq. (1.22) should be small in order to treat the explicit breaking terms given in Eq. (1.20) as a perturbation. The scalar mass spectrum is also modified by the first term in Eq. (1.20) and we obtain

$$\begin{aligned}
m^2_{\sigma_\pi} &= m^2_\pi + \tfrac{2}{3}(m^2_K - m^2_\pi)\frac{(\Delta-\sqrt{2})^2}{\Delta(2\Delta+\sqrt{2})}, \\
m^2_{\sigma_K} &= m^2_\pi + \tfrac{1}{3}(m^2_K - m^2_\pi)\left(\frac{\Delta+2\sqrt{2}}{\Delta}\right), \\
m^2_{\sigma_\eta} &= m^2_\pi + \tfrac{1}{3}(m^2_K - m^2_\pi)\frac{(4+14\sqrt{2}\,\Delta+11\Delta^2)}{\Delta(2\Delta+\sqrt{2})}, \\
m^2_{\pi_{\eta'}} &= m^2_{\sigma_\pi}.
\end{aligned} \tag{1.23}$$

The last relation in Eq. (1.23) indicates an ideal mixing in the $\sigma_\eta - \sigma_{\eta'}$ system:

$$\sigma_{\pi^0} = \frac{1}{\sqrt{2}}(u\bar{u} - d\bar{d}), \quad \sigma_{\eta'} = \frac{1}{\sqrt{2}}(u\bar{u} + d\bar{d}), \quad \sigma_\eta = -s\bar{s} \tag{1.24}$$

just like in the $\omega - \phi$ vector system ($m_\omega = m_\varrho$). An estimate of the Δ-parameter defined in Eq. (1.22) would enable us to predict the full scalar mass spectrum.

Let us consider for that purpose the coupling to a left-handed gauge current. In the QCD Lagrangian given in Eq. (1.1), we have to replace the usual derivative by

a covariant one

$$D_\mu \equiv \partial_\mu - igW_\mu \tag{1.25}$$

and we obtain

$$\mathscr{L}(\text{quarks}) \ni \bar{q}_L(i\not{D})q_L - \tfrac{1}{4} F^L_{\mu\nu}F^{\mu\nu}_L, \tag{1.26}$$

with $F^L_{\mu\nu} = \partial_\mu W_\nu - \partial_\nu W_\mu - ig[W_\mu, W_\nu]$, the field strength tensor. The Lagrangian in (1.26) is invariant under the *local* transformations

$$q_L \to g_L(x)q_L,$$

$$W_\mu \to \frac{i}{g} g_L(x)\partial_\mu g_L^+(x) + g_L(x)W_\mu g_L^+(x) \tag{1.27}$$

and contains the interaction

$$\mathscr{L}(\text{quark}) \ni g\bar{q}^a_L \gamma_\mu W^{ab}_\mu q^b_L. \tag{1.28}$$

On the other hand, the same procedure applied to the linear σ-model defined in Eq. (1.15) gives

$$\mathscr{L}(\text{meson}) \ni i\frac{g}{2} \operatorname{Tr}(\partial_\mu \chi \chi^+ - \chi \partial_\mu \chi^+) W^\mu. \tag{1.29}$$

The identification of Eqs. (1.28) and (1.29) implies therefore the following expression for the left-handed currents

$$J^{ab}_\mu \equiv \bar{q}^a_L \gamma_\mu q^b_L = \frac{i}{2}(\partial_\mu \chi \chi^+ - \chi \partial_\mu \chi^+)^{ba} \ni -\tfrac{1}{4}(\partial_\mu \pi \sigma + \sigma \partial_\mu \pi)^{ba}. \tag{1.30}$$

In the SU(3)-limit (see Eq. (1.18)), we can estimate the π-to-vacuum hadronic matrix element

$$\langle 0|J^{ud}_\mu|\pi^+\rangle = \frac{i}{2} f p_\mu \tag{1.31}$$

measured in the $\pi^+ \to \mu^+\nu$ weak decay (see Fig. 8). Consequently, the vacuum expectation of the σ-field can be related to the pion decay constant:

$$f = f_\pi \simeq 132 \text{ MeV}. \tag{1.32}$$

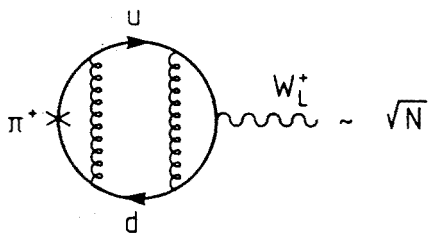

Fig. 8. A planar diagram associated with the π decay constant f_π. The cross denotes the projection on the color-singlet meson bound-state

In the same way, the SU(3)-breaking given in Eq. (1.22) implies a splitting among the pseudoscalar decay constants:

$$\frac{f_K}{f_\pi} = \frac{1+\dfrac{\Delta}{2\sqrt{2}}}{1-\dfrac{\Delta}{\sqrt{2}}}. \tag{1.33}$$

Notice that $\Delta = -2\sqrt{2}$, i.e. $f_K = 0$, corresponds to the non-realistic chimeral solution given in Eq. (1.17).

The SU(3) breaking parameter Δ is a function of measured pseudoscalar decay constants. The ratio given in Eq. (1.33)) can indeed be extracted from the K^+ and π^+ leptonic decays:

$$\frac{f_K}{f_\pi} = \left\{\frac{m_\pi \Gamma(K^+ \to \mu^+ \nu)}{m_K \Gamma(\pi^+ \to \mu^+ \nu)}\right\}^{1/2}$$

$$\times \left\{\frac{1-\left(\dfrac{m_\mu}{m_\pi}\right)^2}{1-\left(\dfrac{m_\mu}{m_K}\right)^2}\right\} \times \frac{V_{ud}}{V_{us}} \simeq 0.275 \frac{V_{ud}}{V_{us}}. \tag{1.34}$$

The Kobayashi-Maskawa mixing matrix elements V_{ij} appearing in (1.34)

$$V_{ud} \simeq 0.975, \quad V_{us} \simeq 0.22 \tag{1.35}$$

are estimated from nuclear β-decays and $K \to \pi e \nu$, respectively [14]. We obtain then the ratio [15]

$$\frac{f_K}{f_\pi} = 1.22 \pm 0.01 \tag{1.36}$$

namely (see Eq. (1.33)) a small SU(3) breaking effect

$$\Delta \simeq 0.18 \ll 1 \tag{1.37}$$

as it should be. Combining the results obtained in Eqs. (1.23), (1.33) and (1.36), we can now plot the scalar mass spectrum as a function of f_K/f_π (see Fig. 9). We have also indicated the scalar resonances reported in the Review of Particle Properties, April 1988. An ideal mixing picture for the scalars clearly favors the assignements $\sigma_\pi = a_0(980)$, $\sigma_{\eta'} = f_0(975)$ and $\sigma_\pi = f_0(1590)$ but excludes the $f_0(1400)$ resonance from the lowest-lying scalar nonet. However, the large $f_0(975) \to K\bar{K}$ measured branching ratio remains puzzling. We also notice that a scalar-glueball mixing invoked sometimes to explain the scalar mass spectrum, is color-suppressed in the framework of the $\dfrac{1}{N}$ expansion.

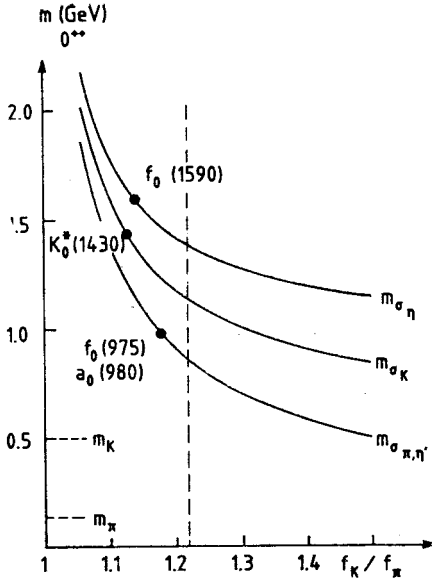

Fig. 9. The scalar mass spectrum obtained in the linear σ-model (1.15), as a function of the ratio $\frac{f_K}{f_\pi}$. The vertical dashed-line stands for the experimental value of this ratio (see Eq. (1.36)). The dots represent a possible assignment of observed scalar resonances

The decay widths of the scalars can also be estimated in the linear σ-model. For that purpose, it is useful to make the following change of variables (polar theorem):

$$\chi \equiv \xi(\pi)\frac{\sigma}{\sqrt{2}}\xi(\pi); \quad \xi(\pi) = \exp\left(\frac{i\pi}{\sqrt{2}f}\right) \tag{1.38}$$

to rotate away the pseudoscalar π fields in the potential of the linear σ-model (see Eq. (1.15)).

The linear transformation of χ under G_f (see Eq. (1.13)) implies

$$\xi \to g_L \xi h^+ = h\xi g_R^+, \quad \sigma \to h\sigma h^+, \tag{1.39}$$

with h, a complicated non-linear function of $g_{L,R}$ and π. However, taking $h = g_L = g_R$, we notice that the π and σ nonets still transform linearly under the flavor $U(3)_V$ symmetry, as it should be.

In the SU(3) limit (see Eq. (1.18)), the change of variable (1.38) in the kinetic term of the linear σ model induces the following simple scalar-pseudoscalar interactions:

$$\frac{f}{2\sqrt{2}}\,\mathrm{Tr}\,\partial_\mu U \partial_\mu U^+ (\xi\tilde{\sigma}\xi^+); \quad \tilde{\sigma} = \sigma - \langle\sigma\rangle, \tag{1.40}$$

with

$$U \equiv \xi\xi = \exp\left(\frac{i\sqrt{2}\,\pi}{f}\right). \tag{1.41}$$

Taking into account the $\eta-\eta'$ mixing (see below), we derive from Eq. (1.40) the decay width

$$\Gamma(a_0 \to \eta\pi) \simeq 400 \text{ MeV} \tag{1.42}$$

which is a factor eight larger than the present experimental value. Further theoretical as well as experimental investigations are needed to settle this puzzle.

In conclusion, the renormalizable linear σ-model provides a nice effective description of the chiral symmetry breaking in terms of mesons. However, the predicted scalar mass spectrum around one GeV (see Fig. 9) and large decay rates are not in full agreement with the present data. It is therefore preferable to restrict ourselves to an effective theory valid below one GeV, such that the scalars essentially decouple.

2. The non-linear σ-model and the quark mass ratios

The non-linear σ-model truncated to the pseudoscalars is simply derived from the linear Lagrangian of Eq. (1.15) by freezing the scalar degrees of freedom. Using the change of variables given in Eq. (1.38) and replacing σ by its vacuum expectation value, $\langle\sigma\rangle = \frac{f}{\sqrt{2}} 1$, we obtain

$$\mathscr{L}_{\text{NL}} = \frac{f^2}{8}\{\text{Tr}\,\partial_\mu U \partial_\mu U^+ + r\,\text{Tr}\,m(U+U^+)$$

$$+ \frac{\alpha}{4N}[\text{Tr}\,(\ln U - \ln U^+)]^2\}, \tag{2.1}$$

with m, the diagonal quark mass matrix defined in (1.21) and $U(\pi)$ given in Eq. (1.41). A straightforward identification of the mass terms in Eqs. (2.1) and (1.1) gives

$$\bar{q}_R^a q_L^b = -\frac{f^2 r}{8} U^{ba} \tag{2.2}$$

such that the parameter r is related to the $q\bar{q}$ condensate estimated in Eq. (1.8):

$$r = -\frac{4\langle q\bar{q}\rangle}{f^2} \simeq 4 \text{ GeV}. \tag{2.3}$$

We notice that the relation

$$\frac{\langle q\bar{q}\rangle}{1 \text{ GeV}} \sim f^2 \tag{2.4}$$

is consistent with the $\frac{1}{N}$ expansion. The N-dependence of the pseudoscalar decay constant is indeed given by

$$f \sim N \cdot N^{-1/2} = \sqrt{N} \tag{2.5}$$

the factor N due to the quark loop in Fig. 8 being partially compensated by the usual normalization factor $N^{-1/2}$ associated with a color-singlet meson-state.

The Lagrangian of Eq. (2.1) provides a very elegant way to incorporate the constraints of current algebra for the light pseudoscalars π_a [16]. For illustration, let us consider the pseudoscalar mass spectrum. Expanding the exponential U up to the second order, we find:

$$m^2_{K^0} = \frac{r}{2}(m_s+m_d),$$

$$m^2_{K^+} = \frac{r}{2}(m_s+m_u),$$

$$m^2_{\pi^+} = \frac{r}{2}(m_u+m_d),$$

$$m^2_{\pi^0} \simeq \frac{r}{2}(m_u+m_d) - \tfrac{1}{2}\frac{\left[\frac{r}{2}(m_u-m_d)\right]^2}{m^2_{\eta'}}, \tag{2.6}$$

where the second term in the π^0 squared mass arises from the isospin-breaking $\pi^0-\eta$ mixing.

The isospin-breaking effects induced by electromagnetism must be under control to estimate the quark (current) mass ratios from Eq. (2.6). In the non-linear σ-model, the couplings to electromagnetism are simply introduced in the Lagrangian (2.1) by means of the covariant derivative

$$D_\mu U = \partial_\mu U - ieB^{e.m}_\mu [Q, U], \tag{2.7}$$

with $Q = \text{diag}\,(\frac{2}{3}, -\frac{1}{3}, -\frac{1}{3})$, the quark electric charge matrix. The commutator appearing in Eq. (2.7) is due to the fact that the photon couples equally to left and right-handed quark fields. The derivation of the current algebra theorems for electromagnetic interactions becomes then straightforward. For example, the Sutherland theorem [17] on the vanishing of the leading electromagnetic contribution to the isospin-violating $\eta \to \pi\pi\pi$ process is left as an exercise. In the same way, it is easy to reproduce the Dashen theorem [18] for the pseudoscalar mass splittings:

$$(m^2_{K^+} - m^2_{K^0})_{QED} = (m^2_{\pi^+} - m^2_{\pi^0})_{QED}. \tag{2.8}$$

This result allows a safe estimate of the isospin breaking in the quark masses:

$$\frac{r}{2}(m_d - m_u) \simeq m^2_{K^0} - m^2_{K^+} - (m^2_{\pi^0} - m^2_{\pi^+})$$

$$\simeq 0.0053\ \text{GeV}^2, \tag{2.9}$$

and consequently, a determination of the quark current mass ratios [19]

$$\frac{m_u}{m_d} \sim 0.55, \quad \frac{m_s}{m_d} \sim 20.1. \tag{2.10}$$

In the isospin limit, the $\eta_8 - \eta_0$ squared mass matrix reads

$$\begin{pmatrix} \frac{1}{3}(4m_K^2 - m_\pi^2) & -\frac{2\sqrt{2}}{3}(m_K^2 - m_\pi^2) \\ -\frac{2\sqrt{2}}{3}(m_K^2 - m_\pi^2) & \frac{1}{3}(2m_K^2 + m_\pi^2) + \alpha \end{pmatrix} \tag{2.11}$$

and contains the SU(3) Gell-Mann-Okubo relation

$$m_{88}^2 = \tfrac{1}{3}(4m_K^2 - m_\pi^2). \tag{2.12}$$

The physical η and η' eigenstates are obtained after diagonalization of the two-by-two matrix in Eq. (2.11):

$$\eta = \eta_8 \cos\theta - \eta_0 \sin\theta, \quad \eta' = \eta_8 \sin\theta + \eta_0 \cos\theta, \tag{2.13}$$

with

$$\begin{aligned} \operatorname{tg} 2\theta &\equiv \frac{2m_{80}^2}{m_{00}^2 - m_{88}^2} \\ &= 2\sqrt{2}\left\{1 - \frac{3\alpha}{2(m_K^2 - m_\pi^2)}\right\}^{-1}. \end{aligned} \tag{2.14}$$

For $\alpha = 0$, we obtain the ideal mixing $\theta \sim 35°$ and consequently the mass relation $m_{\eta'} = m_\pi$ at the source of the so-called $U(1)_A$ problem [20]. Using the trace condition $\alpha = m_{\eta'}^2 + m_\eta^2 - 2m_K^2$, one finds that the observed mass of the η' pseudoscalar requires [13] in fact a rather large value for α:

$$\alpha \sim 0.72\ \text{GeV}^2. \tag{2.15}$$

From Eq. (2.14) we then conclude that

$$\theta \simeq -19° \tag{2.16}$$

in good agreement with the experimental data [21].

However, the popular way to extract this $\eta - \eta'$ mixing is based on the 8–8 matrix element

$$\operatorname{tg}\theta_2 = -\left\{\frac{m_{88}^2 - m_\eta^2}{m_{\eta'}^2 - m_{88}^2}\right\}^{1/2}. \tag{2.17}$$

In this way, the resulting value

$$\theta_2 \simeq -10° \tag{2.18}$$

is obviously very sensitive to any departure from the Gell-Mann-Okubo (GMO) relation originally derived in the octet approximation ($m_{88} = m_\eta$). We conclude that sizeable chiral corrections are needed to get a consistent derivation of the $\eta - \eta'$ mixing θ.

In fact the study of the pseudoscalar decay constants leads to a similar conclusion. Introducing the covariant derivative

$$D_\mu U = \partial_\mu U - igW_\mu U \tag{2.19}$$

in the Lagrangian (2.1) of the non-linear σ-model, we obtain indeed the SU(3)-invariant weak currents

$$J_\mu^{ab} = \frac{if^2}{4} (\partial_\mu U U^+)^{ba} \tag{2.20}$$

such that $f_K = f_\pi$.

Let us therefore consider the following SU(3)-breaking redefinition of the pseudoscalar fields.

$$U \to U' = U + d[m(x) - Um^+(x)U] \tag{2.21}$$

which preserves the unitarity of U up to second order in the quark mass matrix m. This transformation applied on the leading Lagrangian (2.1) gives

$$\delta\mathscr{L}^{(0)} = -\frac{df^2}{8} \operatorname{Tr} \{2m^+ U\partial_\mu U^+ \partial_\mu U + 2m\partial^2 U^+ + rmU^+ mU^+ - rmm^+ + \text{h.c.}\}. \tag{2.22}$$

Consequently, for a specific choice of the parameter d, the next-to-leading (in chiral perturbation), SU(3) non-invariant, effective Lagrangian can be parametized in terms of three independent operators only

$$\mathscr{L}_m^{(1)} = \frac{f^8}{8} \operatorname{Tr} \left\{ -\frac{r}{\Lambda_0^2} m\partial^2 U^+ + \frac{4r^2}{\Lambda^2} mU^+ mU^+ - \frac{4r^2}{\Lambda'^2} mm^+ + \text{h.c.} \right\} \tag{2.23}$$

such that tedious wave-function renormalizations are avoided.

The first effective operator induces the needed SU(3)-breaking corrections to the weak currents:

$$\delta J_\mu^{ab} = -i\frac{f^2}{8} \frac{r}{\Lambda_0^2} (m\partial_\mu U^+ - \partial_\mu U m)^{ba} \tag{2.24}$$

such that

$$\frac{f_K}{f_\pi} = 1 + \frac{(m_K^2 - m_\pi^2)}{\Lambda_0^2} + O\left(\frac{1}{\Lambda_0^4}\right). \tag{2.25}$$

It is worth comparing this relation with the expression derived in the framework of the linear σ-model (see first Section). Expanding indeed Eq. (1.33) to the first-order in the SU(3)-breaking parameter Δ and inserting the first mass relation of Eq. (1.23), we obtain

$$\frac{f_K}{f_\pi} \simeq 1 + \frac{3}{2\sqrt{2}} \Delta = 1 + \left(\frac{m_K^2 - m_\pi^2}{m_{\sigma_\pi}^2 - m_\pi^2} \right). \tag{2.26}$$

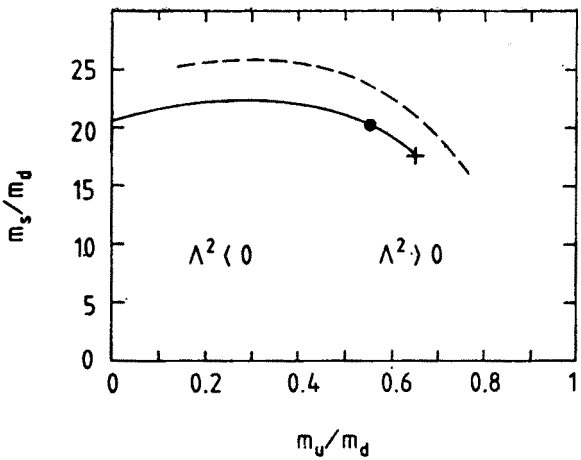

Fig. 10. The quark current-mass ratios m_u/m_d vs m_s/m_d by restricting the second-order chiral corrections to the squared pseudoscalar masses to be less than 25%. The dashed curve is taken from Ref. [22]. The full curve represents the large-N approximation with $|\Lambda| \geqslant 1$ GeV. The heavy dot stands for the first-order determination ($|\Lambda| = \infty$). The cross denotes the second-order estimate ($\Lambda = 1$ GeV)

The chiral symmetry-breaking scale Λ_0, introduced as a correction to the non-linear σ-model, is essentially the scalar mass derived in the linear σ-model.

$$\Lambda_0 \simeq m_{\sigma_\pi} \simeq 1 \text{ GeV}. \tag{2.27}$$

The second effective operator in Eq. (2.23) provides the chiral corrections to the pseudoscalar masses. In the isospin limit, we find

$$M^2_{K,\pi} = m^2_{K,\pi}\left(1 + \frac{m^2_{K,\pi}}{\Lambda^2}\right) \tag{2.28}$$

such that corrections of about 25% are also expected for $\Lambda^2 \simeq \pm 1$ GeV^2. Keeping isospin-breaking terms and taking into account the leading electromagnetic corrections for the charged pseudoscalars, we obtain the relations:

$$M^2_{K^+} - M^2_{\pi^+} \simeq u\left\{1 - y + \frac{u}{\Lambda^2}(1+2x)\right\},$$

$$M^2_{K^0} \simeq u\left\{1 + y + \frac{u}{\Lambda^2}(1+2y)\right\},$$

$$M^2_{\pi^0} \simeq u\{x+y\}, \tag{2.29}$$

with $2u = rm_s$, $x = m_u/m_s$ and $y = m_d/m_s$. Eq. (2.29) contains four parameters (u, x, y and Λ) for fitting three combinations of pseudoscalar masses. We obtain then Fig. 10 which displays the current-mass ratios m_u/m_d vs m_s/m_d as a function of the chiral symmetry-breaking scale Λ. A comparison with the curve displayed in Ref. [22], where next-to-

-leading (in the $\frac{1}{N}$ expansion) loop-effects are included, indicates that the large-N limit provides a good and useful approximation to describe the pseudoscalar mass spectrum. In particular, a massless up quark appears for $\Lambda^2 \simeq -1$ GeV^2. Such a surprising possibility would automatically solve the so-called strong CP problem without the need of an elusive axion.

However, our simpler approach allows a determination of the sign as well as the magnitude of Λ^2 from the study of the $\eta-\eta'$ mixing [23]. The second-order GMO relation reads

$$M_{88}^2 = \tfrac{1}{3}\left\{2(m_{K^+}^2 - M_{\pi^+}^2) + 2M_{K^0}^2 + M_{\pi^0}^2 + \frac{1}{\Lambda^2}(M_{K^+}^2 - M_{\pi^+}^2 + M_{K^0}^2 - M_{\pi^0}^2)^2\right\}. \tag{2.30}$$

The negative $\eta-\eta'$ mixing angle requires $M_{88}^2 > M_\eta^2$ and consequently a *positive* Λ^2 around its expected magnitude. Fig. 11 displays the large chiral correction to the θ_2 angle due to its dependence on the small quantity $M_{88}^2 - M_\eta^2$. Contrary to θ_2, the θ_1 angle gets the typical 25% correction observed in the isosinglet pseudoscalar squared masses. For $\Lambda = 1$ GeV, we obtain now a rather consistent estimate for the $\eta-\eta'$ mixing in the large-N limit, namely (see Fig. 11)

$$\theta_{1,2} = -(22 \pm 2)^0 \tag{2.31}$$

in a good agreement with experimental data.

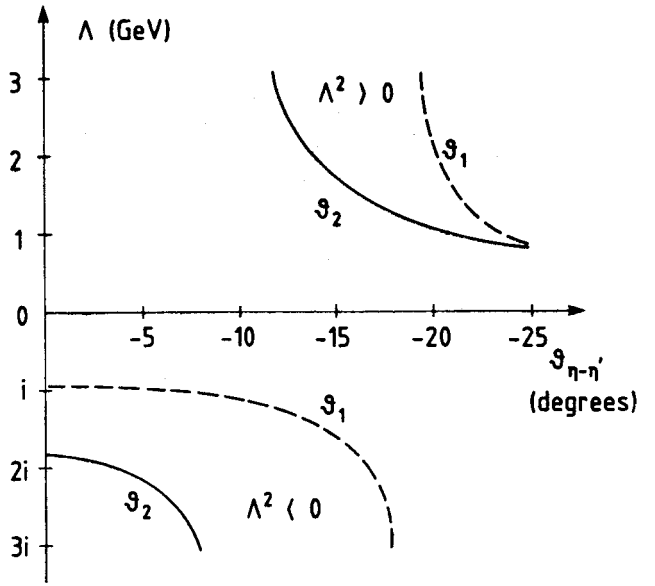

Fig. 11. The $\eta-\eta'$ mixing angle as a function of the chiral symmetry-breaking scale Λ. The dashed (full) curves display the second-order corrections to $\theta_1 \simeq -19°$ and $\theta_2 \simeq -10°$ respectively

Knowing the sign and the magnitude of A^2, we are now able to estimate the light quark mass ratios. From Fig. 10, we can exclude the possibility of a massless up quark and conclude that second-order corrections to the Weinberg mass ratios given in Eq. (2.10) are relatively small. For $A = 1$ GeV, we find indeed [23]

$$\frac{m_u}{m_d} \simeq 0.66, \quad \frac{m_s}{m_d} \simeq 17.7. \tag{2.32}$$

Absolute predictions on the size of the light quark masses require technics beyond chiral perturbation. Non-perturbative methods based on QCD sum rules provide [24] estimates for these masses. The $\frac{1}{N}$ expansion applied to the $\pi^+ - \pi^0$ mass difference gives also a prediction for the light quark masses for the following reason.

The Eqs. (2.6) and (2.9) imply that the $\pi^+ - \pi^0$ mass difference due to the isospin violation in the up-down quark mass

$$(m_{\pi^+} - m_{\pi^0})_{QCD} = O(-0.1 \text{ MeV}) \tag{2.33}$$

is negligible compared to the measured one

$$(m_{\pi^+} - m_{\pi^0})^{exp} \simeq 4.6 \text{ MeV}. \tag{2.34}$$

Electromagnetism must therefore be the main source of the $\pi^+ - \pi^0$ mass splitting, and the virtual photon can be used as a probe to study hadronic physics. In particular, an estimate of the $q\bar{q}$ condensate, and consequently of the parameter r (see Eq. (2.3)), is possible.

3. The $\pi^+ - \pi^0$ electromagnetic mass difference

Let us first estimate this mass-splitting in the framework of the effective meson theory truncated to the pseudoscalars and defined by Eqs. (2.1) and (2.7). At the order α_{QED}, the electromagnetic corrections to the π^+ mass is simply given by the diagrams of Fig. 12.

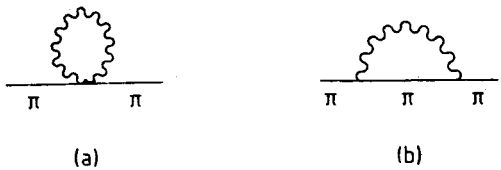

Fig. 12. The Feynman diagrams contributing to the long-distance part of the $\pi^+ - \pi^0$ electromagnetic mass difference in the low-energy truncation with only pseudoscalar mesons

Working with the ξ-gauge, the propagator of the photon reads

$$(-i)\left(g_{\mu\nu} - \xi \frac{q_\mu q_\nu}{q^2}\right)\Big/ q^2. \tag{3.1}$$

A straightforward calculation gives then the following gauge-independent result in the chiral limit ($m_\pi^2 \to 0$):

$$\Delta m_\pi^2(0^{-+}) = \frac{3}{4\pi}\alpha_{\rm QED}\int_0^{M_2} dq^2, \tag{3.2}$$

with q^2, the photon-momentum running in the loop and M, the Euclidean ultraviolet cut-off associated with the truncation of the meson theory. We notice that for $\xi = 1(4)$, only the first (second) diagram of Fig. 12 contributes to the $\pi^+ - \pi^0$ mass difference. The experimental mass splitting could be reproduced for the reasonable cut-off scale $M \sim 0.85$ GeV. However, physics has no reason to stop at this particular scale. In fact,

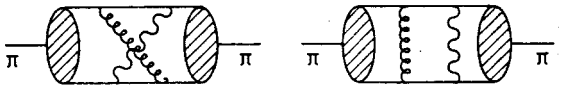

(a) (b)

Fig. 13. The Feynman diagrams contributing to the short-distance part of the $\pi^+ - \pi^\circ$ electromagnetic mass difference in perturbative QCD

the contributions arising from large-q^2 loop-momenta can be estimated in the framework of perturbative QCD.

At small distance, say $q^2 > 1$ GeV^2, the order $\alpha_{\rm QCD}$ contributions to the $\pi^+ - \pi^0$ electromagnetic mass difference are simply given by the diagrams of Fig. 13. In the large-N limit (see Appendix A), we find

$$\Delta m_\pi^2 \,(\text{pert. QCD}) = \tfrac{3}{8}\alpha_{\rm QED} f^2(\alpha_{\rm QCD} r^2)\int_{M_2}^{\infty}\frac{dq^2}{q^4}, \tag{3.3}$$

with M acting now as an infrared cut-off associated with the truncation of the QCD theory. The running QCD coupling is given by

$$\alpha_{\rm QCD}(\mu) = \frac{6\pi}{(11N-2n)\log\dfrac{\mu}{\Lambda_{\rm QCD}}}, \tag{3.4}$$

with μ, the normalization scale at which r, or equivalently the light quark masses (see Eq. (2.6)):

$$\hat{m}(\mu) \equiv \tfrac{1}{2}(m_u + m_d)(\mu) = \frac{m_{\pi^0}^2}{r(\mu)} \tag{3.5}$$

is estimated. In these lectures, $\Lambda_{\rm QCD}$ is defined for three flavors ($n = 3$).

Our phenomenological intuition tells us that strong interactions can, in principle,

be described either in terms of mesons or in terms of the quark and gluon degrees of freedom. Let us therefore assume that the meson theory truncated to the pseudoscalars and perturbative QCD provide *complementary pictures* for strong interactions below and above $M \sim 1$ GeV, respectively. In that case, we can simply add the expressions given in Eqs. (3.2) and (3.3) to obtain the $\pi^+ - \pi^0$ mass splitting since the q^2 loop-momentum carried by the virtual mesons in Fig. 12 is identical to the q^2 loop-momentum of the gluon in Fig. 13:

$$q^2_{\text{meson}} = q^2_{\text{quark-gluon}} = q^2_{\text{photon}}. \tag{3.6}$$

Defining the cut-off M to be the scale at which the integrands in Eqs. (3.2) and (3.3) are equal, we obtain [25] the reasonable values $M = 0.7(0.6)$ GeV for $\hat{m}(1\text{ GeV}) = 4.6(6.9)$ MeV, respectively.

Fifty percent of the total contribution to the $\pi^+ - \pi^0$ mass splitting Δm arises from "physics below one GeV". We find $\Delta m = 6.4(4.3)$ MeV if $\Lambda_{\text{QCD}} = 0.3$ GeV and $\Delta m = 5.5(3.7)$ MeV if $\Lambda_{\text{QCD}} = 0.2$ GeV. These values for Δm are in fair agreement with the "observed" mass difference [26]

$$\Delta m^{\text{exp}} = (4.43 \pm 0.03)\text{ MeV} \tag{3.7}$$

obtained after substraction of the small effects due to the $(m_d - m_u)$ quark mass difference (see for example Eq. (2.6)).

The severe truncation of the meson theory to the pseudoscalars represents a good first step. However, a comparison between Eqs. (3.2) and (3.3) indicates a rather strong dependence on M^2. In other words, the transition from perturbative QCD $\left(\sim \frac{1}{q^4}\right)$ to the meson theory truncated to the pseudoscalars (~ 1) is too sharp. Is our phenomenological intuition wrong? Once again, the answer can be found in the framework of the $\frac{1}{N}$ expansion [6].

Let us indeed consider the two-point function of a current J (see Fig. 14). Using the diagrammatic rules introduced in the first Section, we observe that in the large-N limit, any cut gives only rise to a single intermediate meson state if we assume confinement. A close look at the color index flow in Fig. 14 excludes for example the possibility of a $(\bar{q}_k q^k)\,(G^j_i G^i_j)$ meson-glueball intermediate state. The two-point function can therefore

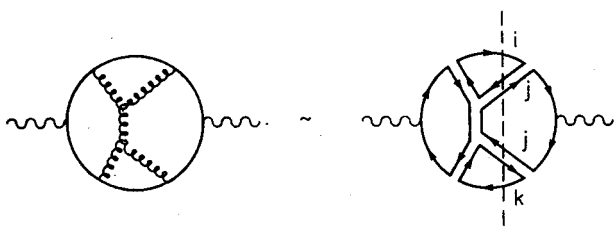

Fig. 14. A typic al contribution to the two-point function in the large-N limit. A cut reveals the intermediate states

be written as a sum over one-meson poles:

$$\langle J(q)J(-q)\rangle = \sum_n \frac{a_n^2}{q^2 - m_n^2} \,. \tag{3.8}$$

On the other hand, perturbative QCD tells us that

$$\langle J(q)J(-q)\rangle \underset{q_2 \to \infty}{\sim} \log q^2. \tag{3.9}$$

The equivalence (duality) between a meson theory for strong interactions and QCD is therefore possible only if the former contains an infinite number of states. A finite sum in Eq. (3.8) could never reproduce exactly the logarithmic behaviour predicted by Asymptotic Freedom, and a matching problem between perturbative QCD $\sim \log q^2$ and the truncated meson theory $\left(\sim \frac{1}{q^2}\right)$ would automatically appear. Similarly, our truncation of the meson theory to estimate the $\pi^+ - \pi^0$ mass splitting is too severe to observe a precocious duality between the two pictures for strong interactions. Heavier state exchange contributions must be included in our calculation.

A chiral model including (axial)-vector mesons is rather easy to build. Let us consider for that purpose the interesting "hidden gauge symmetry approach" of Bando et al. [27]. The basic idea of this approach is to introduce the (axial)-vector mesons as gauge bosons of hidden local symmetry. In the chiral limit, the non-linear σ-model

$$\mathscr{L}(\pi) = \frac{f_\pi^2}{8} \operatorname{Tr} \partial_\mu U \partial_\mu U^+ \tag{3.10}$$

is invariant under the global transformation

$$U \to g_L U g_R^+. \tag{3.11}$$

However, if we define

$$U = \xi(x)\xi(x) = \exp\left(\frac{i\sqrt{2}\,\pi}{f_\pi}\right) \tag{3.12}$$

then

$$\xi \to g_L \xi h^+(x) \equiv h(x) \xi g_R^+, \tag{3.13}$$

with $h(x) \in \mathrm{U(3)_{local}}$ is also symmetry of the Lagrangian. This local symmetry can be gauged by introducing a vector (1^{--}) nonet $V_\mu \equiv \frac{\lambda_a}{2} V_\mu^a$ transforming like

$$V_\mu \to \frac{i}{g} h \partial_\mu h^+ + h V_\mu h^+. \tag{3.14}$$

The Lagrangian becomes then (in the "unitary" gauge)

$$\mathscr{L}(\pi, V) = -\frac{f_\pi^2}{8}\,\mathrm{Tr}\,[\mathscr{D}_\mu\xi^+\xi - \mathscr{D}_\mu\xi\xi^+]^2$$

$$-a\,\frac{f_\pi^2}{8}\,\mathrm{Tr}\,[\mathscr{D}_\mu\xi^+\xi + \mathscr{D}_\mu\xi\xi^+]^2$$

$$-\tfrac{1}{4}\,\mathrm{Tr}\,F_{\mu\nu}F^{\mu\nu} \tag{3.15}$$

with the covariant derivative

$$\mathscr{D}_\mu\xi^{(+)} \equiv \partial_\mu\xi^{(+)} - igV_\mu\xi^{(+)} \tag{3.16}$$

and the non-Abelian field strength tensor

$$F_{\mu\nu} = \partial_\mu V_\nu - \partial_\nu V_\mu - ig[V_\mu, V_\nu]. \tag{3.17}$$

The first term in Eq. (3.15) is equivalent to the pseudoscalar Lagrangian given in Eq. (3.10). The Lagrangian defined in (3.15) has several interesting features. In particular, the comparison between the SU(3)-invariant vector mass

$$m_V = \sqrt{\frac{a}{2}}\,gf_\pi \sim 0.77\ \mathrm{GeV} \tag{3.18}$$

and the $V\pi\pi$ coupling

$$g_{V\pi\pi} = \left(\frac{a}{2}\right)g \sim 6.1$$

indicates that the free-parameter a is close to 2. In fact, the weak left-handed current derived from Eq. (3.15) contains the term

$$J_\mu^{ab} \ni -\left(\frac{a}{2}\right)f_\pi^2 g(\xi V_\mu \xi^+)^{ba} \tag{3.19}$$

such that the decay constant of the ϱ vector-meson can be expressed in terms of the pseudoscalar one. We have indeed

$$\langle 0|J_\mu|\varrho^+\rangle = -\left(\frac{a}{2\sqrt{2}}\right)f_\pi^2 g\varepsilon_\mu$$

$$\equiv -\tfrac{1}{2}f_V m_V \varepsilon_\mu \tag{3.20}$$

namely $f_V = \sqrt{a}f_\pi$. We reproduce the so-called KSRF relation [28]

$$f_V = \sqrt{2}f_\pi \tag{3.21}$$

if

$$a = 2. \tag{3.22}$$

It is also remarkable that vector dominance (no direct $B_\mu \pi \partial_\mu \pi$ coupling) is implemented for this particular value of the parameter a.

The inclusion of the axial-vector (1^{++}) nonet is similar. To extend the local hidden symmetry to $U(3) \times U(3)$, one defines [27]

$$U = \xi_L^+ \xi_M \xi_R \tag{3.23}$$

such that

$$\xi_{L,R} \to h_{L,R}(x) \xi_{L,R} g_{L,R}^+, \quad \xi_M \to h_L(x) \xi_M h_R^+(x) \tag{3.24}$$

leaves $\mathscr{L}(\pi)$ invariant. Gauging this symmetry, one obtains a chiral-invariant Lagrangian for the pseudoscalars, vectors and axial-vectors which contains two additional free-parameters. These two parameters can be determined if the two Weinberg sum rules [29] (see Appendix B) together with Eq. (3.21), namely

$$f_V = \sqrt{2} f_\pi = \sqrt{2} f_A, \quad m_A = \sqrt{2}\, m_V \tag{3.25}$$

are imposed. The couplings to electromagnetism are again introduced by means of the covariant derivative defined in Eq. (2.7). The one-loop (axial)-vector meson contributions

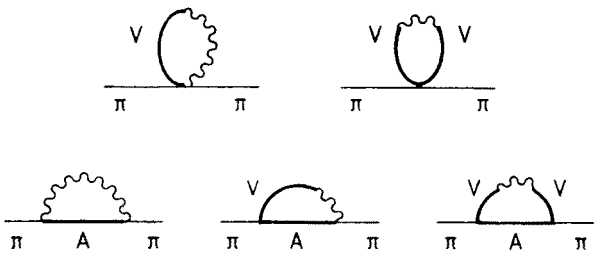

Fig. 15. The pseudoscalar, vector and axial-vector meson next-to-leading contributions to the long-distance part of the $\pi^+ - \pi^\circ$ electromagnetic mass difference in the $\xi = 1$ (Landau) gauge

to the $\pi^+ - \pi^0$ mass splitting (see (Fig. 15)) give then

$$\Delta m_\pi^2(0^{-+}, 1^{--}, 1^{++}) = \frac{3}{4\pi} \alpha_{QED} \int_0^{M^2} dq^2 \frac{m_A^2 m_V^2}{(q^2 + m_A^2)(q^2 + m_V^2)}. \tag{3.26}$$

The same result can be derived [25] in the framework of the "massive Yang-Mills" theory [27] for mesons. If we send the cut-off M to infinity in Eq. (3.26) and assume the second relation in Eq. (3.25), we recover the famous result [30] obtained using current algebra techniques, namely $\Delta m = \frac{3\alpha_{QED}}{4\pi} \frac{m_\varrho^2}{m_\pi} \ln 2 \approx 5.1$ MeV. This rather successful extrapolation from one GeV to infinity requires a huge cancellation [31] among heavier resonance contributions and can only be justified if the large-q^2 corrections are estimated in the framework of perturbative QCD, which is precisely the basic feature of the approach advocated in this Section.

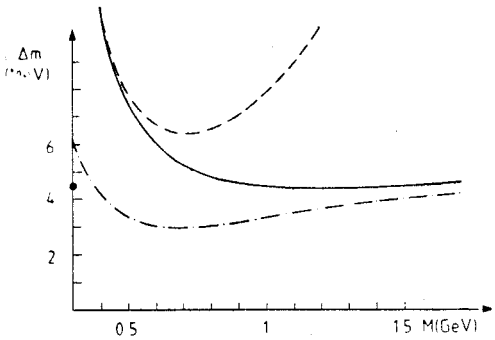

Fig. 16. The $\pi^+ - \pi^0$ electromagnetic mass difference as a function of the cut-off M (scale where we match the meson and quark-gluon pictures). (a) Dashed line: long-distance part calculated with pseudoscalar mesons only and with $\Lambda_{QCD} = 0.3$ GeV, $\hat{m}(1\text{ GeV}) = 4.6$ MeV; (b) Full line: long-distance part calculated with pseudoscalar, vector and axialvector mesons and with $\Lambda_{QCD} = 0.3$ GeV, $\hat{m}(1\text{ GeV}) = 4.6$ MeV; (c) Dashed-dotted line: same as (b) but with $\Lambda_{QCD} = 0.2$ GeV and $\hat{m}(1\text{ GeV}) = 6.9$ MeV. The experimental value is represented by a black dot

In the small-q^2 limit ($q^2 \ll m^2_{V,A}$), Eq. (3.26) simply reduces to the Eq. (3.2). On the other hand, in the large-q^2 limit ($q^2 \gg m^2_{V,A}$), Eq. (3.26) reproduces the q^2-dependence derived from perturbative QCD (see Eq. (3.3)) and confirms our expectation. The inclusion of the (axial)-vector exchange contributions improves indeed the matching between perturbative QCD valid at large q^2 and the meson picture truncated to the pseudoscalar fields valid at small q^2. This implies a better stability of the total $\pi^+ - \pi^0$ mass difference (obtained by adding now Eqs. (3.26) and (3.3)) with respect to cut-off variations around the one GeV scale where both pictures for strong interactions should still be reasonable (see Fig. 16). For $m_A = \sqrt{2} m_V$ and $\hat{m}(1\text{ GeV}) = 4.6(6.9)$ MeV, we obtain [25] respectively

$$\Delta m = 4.4(3.4)\text{ MeV} \quad \text{if} \quad \Lambda_{QCD} = 0.3\text{ GeV},$$
$$\Delta m = 4.0(3.0)\text{ MeV} \quad \text{if} \quad \Lambda_{QCD} = 0.2\text{ GeV} \tag{3.27}$$

to be compared with $\Delta m^{exp} = (4.43 \pm 0.03)$ MeV. We already notice that the solution $\hat{m}(1\text{ GeV}) = 4.6$ MeV with $\Lambda_{QCD} = 0.3$ GeV is prefered. This information turn out to be important for the understanding of the $\Delta I = \frac{1}{2}$ rule and the estimate of the CP-violating parameter ε'/ε (see Sections 5, 6) in the framework of the $\frac{1}{N}$ expansion.

Combining this result with the quark current-mass ratios derived in Section 2, we conclude that

$$m_u(1\text{ GeV}) \cong 3.7\text{ MeV}, \quad m_d(1\text{ GeV}) \cong 5.5\text{ MeV}, \quad m_s(1\text{ GeV}) \cong 100\text{ MeV}, \tag{3.28}$$

for $\Lambda_{QCD} = 0.3$ GeV, to be compared with the standard values [24]

$$m_u(1\text{ GeV}) = (5.1 \pm 1.5)\text{ MeV},$$
$$m_d(1\text{ GeV}) = (8.9 \pm 2.6)\text{ MeV},$$
$$m_s(1\text{ GeV}) = (175 \pm 55)\text{ MeV}. \tag{3.29}$$

To summarize, the real infrared momentum behaviour is determined by the truncated non-linear σ-model which provides about 50% of the $\pi^+ - \pi^0$ mass difference. The vector and axial meson exchanges just modify the q^2-dependence around one GeV to match rather successfully the ultraviolet behaviour controlled by perturbative QCD. A sign of the duality advocated [5, 6] in the framework of $\frac{1}{N}$ expansion is explicitly observed in the case of the $\pi^+ - \pi^0$ electromagnetic mass difference. The virtual photon has been used as a (cheap) probe for strong interactions at small *and* long distances. In the next Sections, we extend this approach to study weak hadronic matrix elements.

4. The $\Delta I = \frac{1}{2}$ rule

At the W-gauge boson mass scale, the $\Delta S = 1$ weak processes are described by the tree-level free-quark diagram given in Fig. 17. The associated effective Hamiltonian is then simply given by

$$H_W^{\Delta S=1} = 2\sqrt{2}\, G_F V_{us} J_\mu^{su} J_\mu^{ud} \equiv \frac{G_F}{\sqrt{2}} V_{us} Q_2^{(q)}(M_W^2), \tag{4.1}$$

with G_F the Fermi constant. To estimate the hadronic matrix elements of this Hamiltonian, we reexpress the left-handed quark current $J_\mu^{aa} = \bar{q}_L^a \gamma_\mu q_L^b$ in terms of meson fields (see

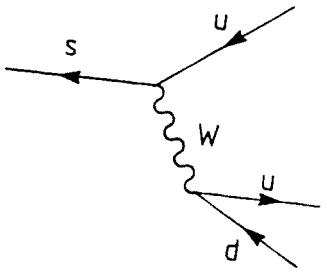

Fig. 17. The $\Delta S = 1$ weak interaction in the free-quark approximation

Eq. (2.20)). In the free-meson approximation, $Q_2^{(q)}(M_W^2) = Q_2^{(\pi)}(0)$ with

$$Q_2^{(\pi)}(0) = -\frac{f^4}{4} (\partial_\mu U U^+)^{du} (\partial_\mu U U^+)^{us} \tag{4.2}$$

and the three $K \to \pi\pi$ decay amplitudes read

$$A(K^0 \to \pi^+\pi^-) = X, \quad A(K^0 \to \pi^0\pi^0) = 0, \quad A(K^+ \to \pi^+\pi^0) = \frac{X}{\sqrt{2}}, \tag{4.3}$$

with $X \equiv \frac{G_F}{\sqrt{2}} V_{us} f_\pi (m_K^2 - m_\pi^2) \simeq 5.5 \cdot 10^{-8}$ GeV. On the other hand, the experimental data

$$A^{exp}(K^0 \to \pi^+\pi^-) \simeq 5.0\,X,$$
$$A^{exp}(K^0 \to \pi^0\pi^0) \simeq 4.8\,X,$$
$$A^{exp}(K^+ \to \pi^+\pi^0) \simeq 0.33\,X \tag{4.4}$$

display a suppression of the pure $\Delta I = \frac{3}{2}$ amplitude $K^+ \to \pi^+\pi^0$ and an enhancement of the $\Delta I = \frac{1}{2}$ component of the $K^0 \to \pi\pi$ amplitudes.

The free-quark and -meson approximations used to derive the theoretical predictions (4.3) implies a factorization of the original Q_2 operator into two currents. These approximations are justified in the large-N limit. In the $\frac{1}{N}$ expansion approach, the short-distance gluon and long-distance meson exchanges between the two currents are indeed $\alpha_s \sim \frac{1}{N}$ and $\frac{1}{f_\pi^2} \sim \frac{1}{N}$ suppressed, respectively. The solution to the so-called $\Delta I = \frac{1}{2}$ rule puzzle within the standard model should therefore arise from the next-to-leading strong interaction corrections.

The following simple observation supports this possibility. Let us consider the one-loop diagram of Fig. 18. This diagram indicates that a non-zero $K^0 \to \pi^0\pi^0$ decay amplitude

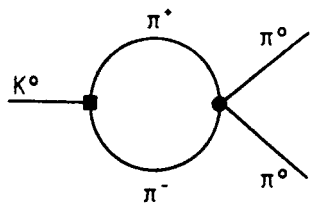

Fig. 18. The one-loop induced $K^0 \to \pi^0\pi^0$ decay diagram. The black box stands for the weak $\Delta S = 1$ Hamiltonian while the black dot represents a strong vertex

is generated by the strong rescattering of the charged pions. In other words, strong interaction corrections to the Q_2 operator induce a new effective current-current meson operator:

$$Q_1^{(\pi)}(0) = -\frac{f^4}{4}(\partial_\mu U U^+)^{ds}(\partial_\mu U U^+)^{uu} \tag{4.5}$$

with $\langle \pi^0\pi^0 | Q_1^{(\pi)} | K^0 \rangle = -\langle \pi^+\pi^- | Q_2^{(\pi)} | K^0 \rangle \neq 0$.

A complete one-loop calculation (see Fig. 19), using the strong Lagrangian (2.1) and the weak currents (2.20) gives the following "meson evolution" in the chiral limit [32]

$$Q_2^{(\pi)}(M^2)_{\frac{1}{N}} = Q_2^{(\pi)}(0) - \frac{4M^2}{(4\pi f_\pi)^2} Q_1^{(\pi)}(0) - \frac{2M^2}{(4\pi f_\pi)^2} \{Q_1 - Q_2\}^{(\pi)}(0). \tag{4.6}$$

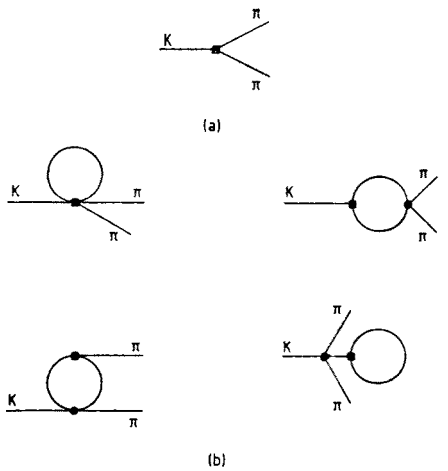

Fig. 19. The (a) leading and (b) next-to-leading contributions to the $\Delta S = 1$ $K \to \pi\pi$ decay amplitudes

Again, a loop-momentum cut-off M is introduced since the meson theory is truncated to the pseudoscalars. The $K \to \pi\pi$ decay amplitudes become then:

$$A(K^0 \to \pi^+\pi^-) = \left\{1 + \frac{2M^2}{(3\pi f_\pi)^2}\right\} X,$$

$$A(K^0 \to \pi^0\pi^0) = \left\{0 + \frac{6M^2}{(4\pi f_\pi)^2}\right\} X,$$

$$A(K^+ \to \pi^+\pi^0) = \left\{1 - \frac{4M^2}{(4\pi f_\pi)^2}\right\} \frac{X}{\sqrt{2}}. \tag{4.7}$$

For $M \simeq 2\pi f_\pi \simeq 0.8$ GeV, the pattern of the experimental decay amplitudes given in Eq. (4.4) can easily be reproduced. In a meson theory truncated to the pseudoscalars, we observe a suppression of the pure $\Delta I = \frac{3}{2}$ amplitude $K^+ \to \pi^+\pi^0$ and an enhancement of the $\Delta I = \frac{1}{2}$ component of the $K^0 \to \pi\pi$ amplitudes.

However, we know that physics does not stop around one GeV and we must include also the next-to-leading corrections arising from larger loop-momenta. The *full* next--to-leading corrections are represented in Figs 20b, c. The factorizable ones simply renormalize the currents appearing in the leading operator (Fig. 20a). There effects are taken into account by including the measured form factors of the $\Delta S = 1$ currents. These corrections as well as the leading contribution were absent in the $\pi^+ - \pi^0$ electromagnetic mass difference, due to spin-parity.

All the next-to-leading nonfactorizable corrections are contained in Fig. 20c. For small photon (W-gauge boson) momenta, the $\pi^+ - \pi^0$ mass difference (the $K \to \pi\pi$ decay amplitudes) have been estimated by means of the truncated meson theory. These are precisely the results presented in Eqs. (3.2) and (4.7) respectively. For large photon (W-gauge boson) momenta, perturbative QCD becomes reliable and the short-distance calculation

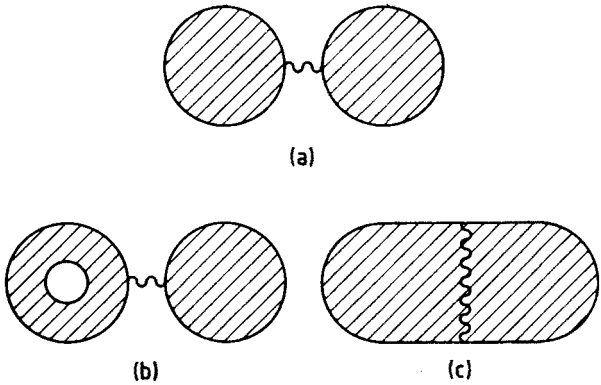

Fig. 20. The complete (a) leading, (b) next-to-leading factorizable and (c) next-to-leading non-factorizable contributions to a weak (electromagnetic) hadronic matrix element. The full line is a quark and the wavy line, a W gauge boson (photon)

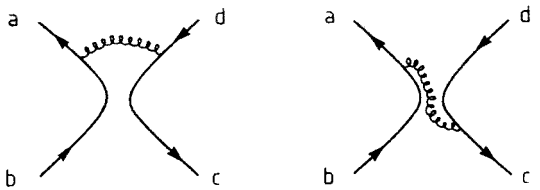

Fig. 21. Short-distance gluonic corrections to a current-current four-quark operator

for the weak decay amplitudes is similar to the one sketched in the Appendix A. Neglecting for a while the so-called "penguin" contributions [33] (see Section 7), the next-to-leading nonfactorizable corrections to a free four-quark current-current operator defined at the W mass scale arise from the gluon exchange from one current to the other one (see Fig. 21) and give [34]

$$J_\mu^{ab} J_\mu^{cd}(M_W^2) = J_\mu^{ab} J_\mu^{cd}(M^2) - \frac{3\alpha_s}{4\pi} \ln\left(\frac{M_W^2}{M^2}\right) J_\mu^{ad} J_\mu^{cb}(M^2). \tag{4.8}$$

In particular, we have the following "quark-gluon evolution"

$$Q_2^{(q)}(M_W^2) = Q_2^{(q)}(M^2) - \frac{3\alpha_s}{4\pi} \ln\left(\frac{M_W^2}{M^2}\right) Q_1^{(q)}(M^2) + \text{"penguin"}. \tag{4.9}$$

Combining Eqs. (4.6) and (4.9) with $Q_2^{(q)}(M) = Q_2^{(\pi)}(M)$, we get a full next-to-leading Q_2 operator evolution from M_W to zero momentum. We notice that the negative "quark--gluon evolution" of Q_2 into Q_1 from M_W to M is consistently extended to lower momenta by a further negative "meson evolution". This remarkable result should be contrasted with the popular vacuum insertion approximation (V.I.A).

The V.I.A consists in inserting the vacuum state in all possible ways in the hadronic matrix element considered, taking into account the Fierz relations given in Eq. (A.3). This approximation provides a simple though unjustified way to express the four-quark

operators defined around one GeV in terms of meson ones at zero momentum. For the Q_2 operator, one finds

$$\langle Q_2^{(q)}(M)\rangle_{VIA} = \langle Q_2^{(\pi)}(0)\rangle + \frac{1}{N}\langle Q_1^{(\pi)}(0)\rangle. \tag{4.10}$$

The factor $\frac{1}{N}$ arises from the projection of the "Fierz induced" Q_1 operator on color-singlet external states. The V.I.A can be viewed as a momentum-independent "evolution". Consequently, the physical amplitudes remain M-dependent (see Eq. (4.9)) and predictions strongly depend on the optimism of the theorist involved. Since the strong coupling α_s becomes large around one GeV, the more you trust perturbative QCD at low scale, the better you can reproduce the empirical $\Delta I = \frac{1}{2}$ rule. Moreover, a comparison between Eqs. (4.9) and (4.10) shows that the low "V.I.A evolution" has the wrong sign and leads to a $\Delta I = \frac{1}{2}$ suppression and a $\Delta I = \frac{3}{2}$ enhancement (see Fig. 22). This flip of sign around one GeV has no physical justification and illustrates the sickness of the V.I.A. In the language of $\frac{1}{N}$ expansion, the V.I.A includes only one part of the next-to-leading terms and is then not consistent.

This observation has also an important implication for the D and B meson weak decays. Of course, an estimate of the "meson evolution" only in terms of the low-lying pseudoscalars does not make much sense for these heavier systems. However, the flip of sign implied by the popular "V.I.A evolution" remains unlikely. It is therefore better

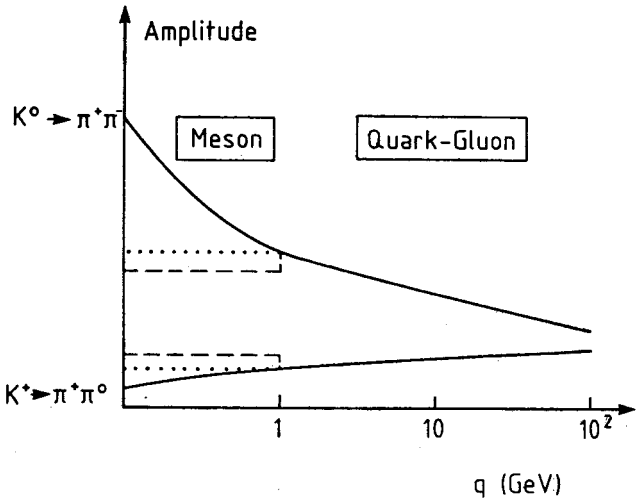

Fig. 22. A sketch (full lines) of the solution to the $\Delta I = \frac{1}{2}$ rule in the $\frac{1}{N}$ expansion approach. The dashed lines correspond to the popular vacuum insertion approximation and the dotted lines, to a large-N approximation for the hadronic matrix elements only

(see Fig. 22) to stay at the leading order in the $\frac{1}{N}$ expansion for the hadronic matrix elements (no evolution at all below the D(B) mass scale) than to include a partial next-to-leading contribution with the wrong sign relative to the known short distance evolution above $m_{D(B)}$. This might explain the rather surprising success of the large-N approximation [35] ($\xi = 0$ procedure [36]) in D-decay amplitudes. If the justification given above is the correct one, the large-N limit should also be successful for the hadronic two-body B-decays.

The results of a complete study of the $K \to \pi\pi$ decay amplitudes at the next-to-leading order in the $\frac{1}{N}$ expansion has been presented in Ref. [32]. In particular, chiral corrections have been included below M and the renormalization group equation has been used [37] above M. The experimental $K \to \pi\pi$ decay amplitudes given in Eq. (4.4) are then reproduced within 30% (see Eq. (7.6)). Consequently, the $\Delta I = \frac{1}{2}$ rule can most probably be explained in the framework of the standard model, although the final answer to this long-standing puzzle requires further investigations inside the physics below one GeV [38].

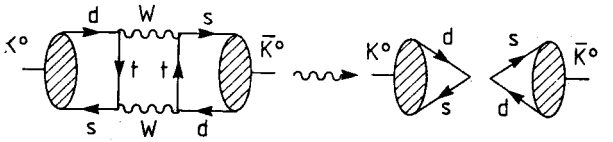

Fig. 23. The box-diagram (and its low-energy representation) responsible for a *CP*-violation in the $K^0 - \bar{K}^0$ mixing

The explanation of the $\Delta I = \frac{1}{2}$ rule in K-decays advocated in Ref. [32] is mainly based on the fact that for low loop-momenta, the logarithmic operator evolution derived [34] within perturbative QCD is turned into a *physical* quadratic one, giving rise to sizeable long distance effects despite the small range of integration. This scenario sketched in Fig. 22 is easy to understand in the framework of the $\frac{1}{N}$ expansion. Perturbative QCD corrections are controlled by the *dimensionless* expansion parameter $\alpha_s \sim \frac{1}{N}$. On the other hand, in the meson theory truncated to the pseudoscalars, the color factor N only appears through the *dimensionful* decay constant f_π (see Eq. (2.5)). Consequently, the long distance expansion parameter must scale like $\frac{q^2}{f_\pi^2} \sim \frac{1}{N}$ in the chiral limit $m_\pi = 0$. The presence of vector mesons around one GeV implies a new (N-independent) dimensionful mass parameter m_V which does not vanish in the chiral limit. The quadratic dependence on the q^2-loop momentum turns then smoothly into a logarithmic one. We expect therefore that the inclusion of heavier resonances just improves the matching around one GeV, in a way very similar to the case of the $\pi^+ - \pi^0$ electromagnetic mass difference treated in the previous Section. The study of the vector meson loop-effects on another important weak hadronic matrix element confirms our expectation.

5. The B-parameter

The well-measured ε_K parameter provides a crucial constraint on the standard model for electroweak interactions with three generations of quarks. In this framework indeed, all the *CP*-violating effects must be triggered by the unique phase contained in the Kobayashi-Maskawa mixing matrix. Therefore, the observation of another *CP*-violation in weak processes should in principle settle the question of its origin. It turns out that such a new effect has been measured recently by the NA31 collaboration [39]. Nevertheless, a general consensus among the theorists is still missing. The origin of this controversy is again related to our present inability of treating strong interaction corrections to weak processes below the one GeV confining scale. In other words, an understanding of *CP*-violation in the kaon system also requires non-perturbative methods [4] such as lattice, QCD sum rules or $\frac{1}{N}$ expansion to evaluate the hadronic matrix elements of associated four-quark operators.

In the particular case of the ε_K parameter which describes the *CP*-violation in the $K^0-\bar{K}^0$ oscillations, one obtains an effective $\Delta S = 2$ current-current operator after integration of the (heavy) W-gauge bosons and top quarks (see Fig. 23):

$$O^{(q)}_{\Delta S=2} \equiv [\bar{s}\gamma_\mu(1-\gamma_5)d]^2 = 4J^{sd}_\mu J^{sd}_\mu. \tag{5.1}$$

The hadronic matrix element of this operator is usually parametrized in the following way

$$\langle \bar{K}^0|O^{(q)}_{\Delta S=2}|K^0\rangle \equiv 2\left(1+\frac{1}{N}\right)Bf_K^2m_K^2. \tag{5.2}$$

The decay constant f_K defined by

$$\begin{aligned}\langle 0|J^{sd}_\mu|K^0\rangle &= \langle \bar{K}^0|J^{sd}_\mu|0\rangle^* \\ &= \frac{i}{2}f_K p^K_\mu\end{aligned} \tag{5.3}$$

is measured in $K \to \mu\nu$ leptonic decays (see Eq. (1.34)).

The parameter B introduced in Eq. (5.2) measures in fact the departure from the value obtained using the V.I.A. Inserting the vacuum state in all possible ways and using Eq. (5.3), we obtain [40] indeed

$$\langle \bar{K}^0|O^{(q)}_{\Delta S=2}|K^0\rangle_{VIA} = 2\left(1+\frac{1}{N}\right)f_K^2m_K^2. \tag{5.4}$$

The momentum-independent $\frac{1}{N}$-suppressed contribution is simply induced by the "Fierzed" current-current operator (see Eq. (A.3)) projected on the color-singlet K-states. The V.I.A. evaluates at zero momentum the hadronic matrix element of a four-quark operator only well-defined above the one GeV confining scale. From Eqs. (5.2) and (5.3), we conclude that

$$B_{VIA}(0) = 1. \tag{5.5}$$

We have already stressed in the previous Section that this extrapolation to zero momentum has no theoretical foundation and should at most be considered as an order of magnitude estimate of hadronic matrix elements. But tests of the electroweak standard model require now a better determination of the B-parameter.

Another popular value for the B-parameter has been derived in the framework of chiral perturbation [41]. The weak left-handed currents $J_\mu^{ab} = \bar{q}_L^a \gamma_\mu q_L^b$ transform like $(8_L, 1_R)$ under the chiral $SU(3)_L \times SU(3)_R$ symmetry. Consequently, the (symmetric) effective weak Hamiltonian transforms like either $(8_L, 1_R)$ or $(27_L, 1_R)$ under the same flavor symmetry. Let us now reexpress the weak Hamiltonian in terms of pseudoscalar fields. The simplest object transforming like a left-handed octet is $(\partial_\mu U U^+)_b^a$ and is proportional to the meson current derived in the non-linear σ-model (see Eq. (2.20)). Using then the unitarity of the U matrix, we can build the effective weak Hamiltonian:

$$H_W = \alpha(\partial_\mu U \partial_\mu U^+)_b^a + \beta(\partial_\mu U U^+)_c^a (\partial_\mu U U^+)_b^d + \ldots \tag{5.6}$$

with α and β, arbitrary couplings if non-factorizable effects are important. The dots denote higher derivative operators giving rise to effects which are suppressed by powers of $\frac{m_{K,\pi}^2}{\Lambda^2}$, Λ being the chiral symmetry breaking scale of the order of one GeV. In the leading order in this so-called chiral expansion, the weak Hamiltonian only contains one octet operator (first term in (5.6)) and one 27 operator (second term in (5.6) after substraction of traces and symmetrization over flavor indices). In this limit, the dominant $\Delta I = \frac{1}{2}$ weak operator for the $K^0 - \pi\pi$ decays is contained in the octet term. On the other hand, the $\Delta S = 2$ operator defined in Eq. (5.1) and the $\Delta I = \frac{3}{2}$ operator responsible for the $K^+ \to \pi^+\pi^0$ belong both to the second SU(3)-invariant term in Eq. (5.6). The B-parameter can therefore be expressed in terms of the measured $K^+ \to \pi^+\pi^0$ decay amplitude and takes the following normalization scale-independent value [41, 42]

$$|B_{\text{chiral}}| \simeq \tfrac{1}{3}\,. \tag{5.7}$$

The derivation of Eq. (5.7) has been done assuming flavor-SU(3) invariance. However, we have seen in Section 2 that the observed splitting between the K and π decay constants requires the introduction of next-to-leading (in the chiral expansion) corrections to the Lagrangian (2.1) of the non-linear σ-model.

The large-N limit also implies the absence of short-distance (see Eq. (1.11)) and long-distance (see Eq. (2.5)) strong interaction corrections induced respectively by gluon and meson exchanges between the two currents of the $\Delta S = 2$ operator. Consequently, we have a complete factorization of $O_{\Delta S=2}$ into two currents as well as a control on SU(3) breakings in this limit. Using Eqs. (5.1), (2.20) and (2.24), we finally obtain

$$\begin{aligned} \langle \bar{K}^0 | O_{\Delta S=2}^{(\pi)} | K^0 \rangle &= 2\left(1 + \frac{2m_K^2}{\Lambda_0^2}\right) f^2 m_K^2 \\ &= 2 f_K^2 m_K^2. \end{aligned} \tag{5.8}$$

We conclude then that [43]

$$B_{N\to\infty} = \tfrac{3}{4} \tag{5.9}$$

in the large-N limit. But why is this value precisely lying between the two popular values derived in Eqs. (5.5) and (5.7)?

It is rather easy to understand why the chiral result (5.7) is an underestimate of the B-parameter in the framework of the $\frac{1}{N}$ expansion. If we remove indeed the SU(3)-breaking term given in Eq. (2.24), the predicted value $\frac{3}{4}$ is already suppressed by a factor $\left(\frac{f_\pi}{f_K}\right)^2 \sim \frac{2}{3}$ and we obtain $B_{N\to\infty} \sim \frac{1}{2}$. The remaining numerical difference with the chiral prediction given in (5.7) results from the fact that the $K^+ \to \pi^+\pi^0$ amplitude is also overestimated by a factor $\sim \frac{3}{2}$ if we take the large-N limit in the associated hadronic matrix element.

The V.I.A. result (5.5) includes one next-to-leading $\left(\text{in the } \frac{1}{N} \text{ expansion}\right)$ correction. We must therefore go beyond the leading order to compare Eqs. (5.5) and (5.9) and to justify the large-N prediction.

To estimate the next-to-leading strong interaction corrections to the $\Delta S = 2$ hadronic matrix element, we adopt the same philosophy as for the $\pi^+ - \pi^0$ electromagnetic mass difference (Section 3) and the $\Delta I = \frac{1}{2}$ rule (Section 4). We divide the q^2 loop-integration into two parts by introducing a cut-off M. The integration below M is then made in the truncated meson picture, a good approximation as long as $M < 1$ GeV. On the other hand, the integration above M is carried out within the perturbative quark-gluon picture, the non-perturbative effects being most probably small for $M \geqslant 1$ GeV.

Once again, the effects of the next-to-leading factorizable contributions are taken into account by using the measured form factors of the $\Delta S = 1$ weak current. Let us therefore focus our attention on the next-to-leading non-factorizable contributions. In the quark-gluon picture, they are due to gluon exchanges from one current to the other one (see Fig. 21) and we obtain

$$O^{(q)}_{\Delta S=2}(M_W^2) = \left\{1 - \frac{3\alpha_s}{4\pi} \ln \frac{M_W^2}{M^2}\right\} O^{(q)}_{\Delta S=2}(M^2) \tag{5.10}$$

from the general relation (4.8). We stress again that in the chiral limit, the $\Delta I = \frac{1}{2}$ penguin contributions (see Section 7) are absent for this operator (see Eq. (5.6)).

The further "meson evolution" below M can be estimated in the meson picture truncated (for a while) to the pseudoscalars. The non-factorizable contributions are induced by the exchanges of π-fields between the two currents (see Fig. 24b) and we find [44]

$$O^{(\pi)}_{\Delta S=2}(M^2) = \left\{1 - \frac{4M^2}{(4\pi f_K)^2}\right\} O^{(\pi)}_{\Delta S=2}(0) \tag{5.11}$$

in the chiral limit. The meson one-loop correction to the $\Delta I = \frac{3}{2}$ $K^+ \to \pi^+\pi^0$ decay amplitude (4.7) has the same quadratic dependence on the cut-off M. As we have already explained

(see Eq. (5.6)), this is a consequence of the fact that in the chiral limit, the $\Delta I = \frac{3}{2}$ and $\Delta S = 2$ weak operators belong to the same representation of flavor SU(3). On the other hand, the logarithmic dependence on M induced by chiral corrections are different.

Identifying the quark and meson $\Delta S = 2$ operators at the scale M, we conclude that the negative "quark-gluon evolution" from M_W down to M (Eq. (5.10)) is consistently extended to lower loop-momenta by a further negative "meson evolution" (Eq. (5.11)).

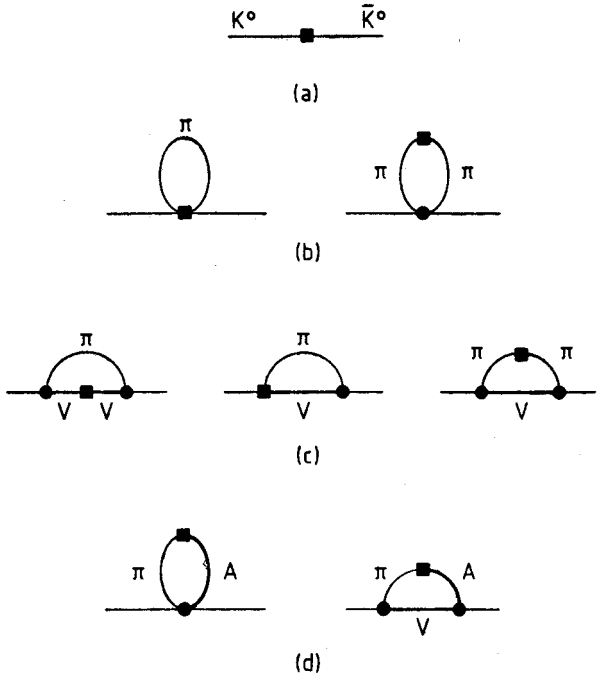

Fig. 24. The (a) leading and the (b) pseudoscalar, (c) vector, (d) axial-vector next-to-leading contributions to the B-parameter. The black box stands for the weak $\Delta S = 2$ Hamiltonian while the black dot represents a strong vertex

This is certainly not the case of the V.I.A. (see (5.4)) which gives again the wrong sign and the wrong momentum dependence for the extrapolation from M to zero. The V.I.A. is obviously an overestimate of the B parameter.

Let us now introduce vector meson exchange contributions to improve the matching between the meson theory evolution ($\sim q^2$) and the perturbative QCD evolution ($\sim \log q^2$) of the $\Delta S = 2$ operator. The new diagrams are given in Fig. 24c and can be estimated within the "hidden gauge symmetry approach" (3.15) of Bando et al. In the chiral limit, we find

$$O^{(\pi,V)}_{\Delta S=2}(M^2) = \left\{1 + \frac{F(M^2)}{(4\pi f_K)^2}\right\} O^{(\pi)}_{\Delta S=2}(0), \tag{5.12}$$

with

$$F(M^2) = (-4+\tfrac{15}{8}\,a-\tfrac{3}{8}\,a^2)M^2$$

$$-\tfrac{3}{8}\,a(5-2a)m_V^2 \ln\left(1+\frac{M^2}{m_V^2}\right)-\tfrac{3}{8}\,a^2 m_V^2\,\frac{M^2}{M^2+m_V^2}\,. \tag{5.13}$$

For $m_V \gg M$, we recover the result (5.11) valid at small momenta. Assuming $a = 2$ (see Eq. (3.22)), we obtain [45]

$$F(M^2) = -\tfrac{7}{4}\,M^2-\tfrac{3}{4}\,m_V^2 \ln\left(1+\frac{M^2}{m_V^2}\right)-\tfrac{3}{2}\,m_V^2\,\frac{M^2}{M^2+m_V^2} \tag{5.14}$$

namely an important modification of the momentum dependence around one GeV. The matching with the logarithmic dependence arising from perturbative QCD is manifestly improved. It results from this a better stability of the B-parameter (and consequently of

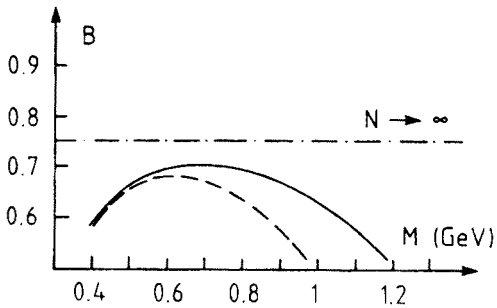

Fig. 25. The B-parameter without (dashed) and with (full) vector meson contributions as a function of the cut-off, for $\Lambda_{QCD} = 0.3$ GeV

the $K^+ \to \pi^+\pi^0$ decay amplitude) with respect to cut-off variations around the vector mass scale. Including chiral corrections ($m_K^2 \neq 0$) below M and using the renormalization group equation to reexpress the short distance evolution (5.10) in terms of the running α_s coupling defined in (3.4), we obtain Fig. 25 for $\Lambda_{QCD} = 0.3$ GeV.

The axial-vector-pseudoscalar $A_\mu V_\mu \pi$ coupling being non-derivative, we do not expect important modifications from axial meson exchanges (see Fig. 24d). In fact an explicit calculation in the framework of the "hidden gauge symmetry" approach extended to a local $U(3)_L \times U(3)_R$ (see Section 3) gives an expression similar to Eq. (5.14) with the factors $-\frac{7}{4}$, $-\frac{3}{4}$ and $-\frac{3}{2}$ replaced by $-\frac{139}{46}$, $-\frac{63}{64}$ and $-\frac{27}{32}$, respectively (in the chiral limit). Consequently, we restrict ourselves to the meson theory truncated to the pseudoscalars and vectors which is more reliable [27].

Contrary to the case of the $\pi^+-\pi^0$ electromagnetic mass difference, (see Eq. (3.6)), the identification of the q^2 loop-momentum of the gluon with the q^2 loop-momentum of the virtual meson, although physical, is not rigorous since the W-gauge bosons are already integrated out (see Fig. 23) in Eq. (5.1). Such an approximation turns out to be quite good in the case of the K_L-K_S mass difference (see next Section). A rescaling of the q^2-mo-

mentum in the quark-gluon picture being equivalent to the inverse rescaling of Λ^2_{QCD} in the running coupling constant $\alpha_s(q^2)$ (see Eq. (3.4)), we try to take this source of uncertainty into account by varying the parameter Λ_{QCD} from 0.1 GeV to 0.4 GeV. The resulting value of the B-parameter is increasing for decreasing Λ_{QCD} and we obtain [45]

$$B_{\frac{1}{N}} = 0.75 \pm 0.15 \tag{5.15}$$

namely a small $\left(\text{next-to-leading in the } \frac{1}{N} \text{ expansion}\right)$ correction to the large-N prediction (5.9). This result has to be compared with the predictions of other nonperturbative methods [46]:

$$\begin{aligned} B_{\text{lattice}} &= 0.8 \pm 0.2, \\ B_{\text{QCD sum rules}} &= 0.5 \pm 0.1 \pm 0.2, \\ B_{\text{hadronic sum rules}} &= 0.33 \pm 0.09. \end{aligned} \tag{5.16}$$

The real discrepancy between (5.15) and the result of hadronic sum rules requires further investigations.

Unfortunately, the B-parameter itself cannot be extracted directly from experimental data. The CP-violating parameter ε_K is indeed proportional to $B \sin \delta_{KM}$, with δ_{KM} the Kobayashi-Maskawa phase, and strongly depends on the top quark mass. Therefore, any prediction on the B-parameter requires an estimate of the measured $K_L - K_S$ mass difference within the *same* non-perturbative framework.

6. *The $K_L - K_S$ mass difference*

Long-distance $\Delta S = 2$ $K^0 - \bar{K}^0$ transitions induced by pion loops are expected to be as large as the typical weak decay width (see Fig. 26a). Consequently, off-diagonal terms arise in the $K^0 - \bar{K}^0$ squared mass matrix and a diagonalization is necessary. The resulting

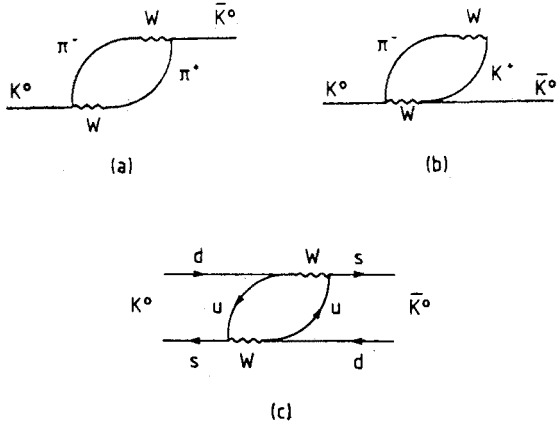

Fig. 26. (a, b) Meson, (c) quark-loop-contributions to the $K_L - K_S$ mass difference

physical eigenstates are then

$$K_L = \frac{1}{\sqrt{2}}(K^0 + \bar{K}^0), \quad K_S = \frac{1}{\sqrt{2}}(K^0 - \bar{K}^0), \tag{6.1}$$

if (tiny) *CP*-violating effects are neglected. The loop-induced $K_L - K_S$ mass splitting Δm being of the second order in the Fermi coupling G_F and in the Cabibbo angle, we define

$$\begin{aligned} \Delta m &\equiv m_L - m_S \\ &\equiv \left(\frac{G_F}{\sqrt{2}}\right)^2 (V_{ud}V_{us})^2 \frac{1}{4\pi^2} f_K^2 m_K M^2 \end{aligned} \tag{6.2}$$

on dimensional grounds (see Fig. 26). Experimentally, the regeneration of the short-lived K_S via matter interactions allows a remarkably precise determination of this mass splitting:

$$\begin{aligned} (\Delta m)_{exp} &= (3.521 \pm 0.014) 10^{-15} \text{ GeV} \\ &\simeq \tfrac{1}{2} \Gamma_S. \end{aligned} \tag{6.3}$$

From Eqs. (6.2) and (6.3), we conclude that

$$M \simeq 1.86 \text{ GeV}. \tag{6.4}$$

The theoretical estimate of this scale M has in fact a very long story which can be sketched in the following way.

In the late sixties, loop calculations supplemented by current algebra techniques [47] led to the suggestion that the weak interaction cut-off M might be identified with the mass of the hypothetical W-gauge boson:

$$M \simeq M_W. \tag{6.5}$$

In 1974, Gaillard and Lee [40] presented their estimate of the quark box-diagram based on the GIM mechanism [48]:

$$M^2 \simeq m_c^2 - m_u^2. \tag{6.6}$$

This theoretical prediction for the charm quark mass was confirmed a few months later with the spectacular discovery of the J/ψ. The magnitude of the $K_L - K_S$ mass difference was eventually understood.

However, the presence of the up quark mass in Eq. (6.6) indicates that long-distance effects induced by pseudoscalar exchanges and loops might be non-negligible [49]. Furthermore, short-distance strong interaction corrections [50] to the box-diagram itself introduce another source of uncertainty:

$$M^2 \simeq \eta_{QCD} m_c^2; \quad 0.7 \leqslant \eta_{QCD} \leqslant 1.0 \tag{6.7}$$

due to our ignorance about the QCD scale ($0.1\ \text{GeV} \leqslant \Lambda_{\text{QCD}} \leqslant 0.3\ \text{GeV}$). Finally, the appearance of a (current or constituent?) strange quark mass dependence in the estimate of the box-diagram with external momenta [51] totally obscures a possible separation of short- and long-distance contributions to Δm:

$$M^2 \simeq m_c^2 + \tfrac{2}{3} m_K^2 \ln \frac{m_c^2}{m_s^2}. \tag{6.8}$$

We have seen in Section 5 that a further uncertainty on the $K_L - K_S$ mass difference arises from the estimate of the hadronic matrix element for the short-distance $\Delta S = 2$ weak operator. The B-parameter measures indeed the deviation from the vacuum insertion approximation used in Ref. [40]. Fifteen years of theoretical investigation led to predictions ranging from $B = -0.4$ to $B = 2.8$. Recently, new non-perturbative techniques have been developped, giving rise to refined estimates. The range

$$1/3 \leqslant B \leqslant 1 \tag{6.9}$$

fairly summarizes the present status of the B-parameter (see Eq. (5.16)).

In the large-N limit, single pseudoscalar exchange contributions and short-distance QCD corrections are $1/N^2$ and $1/N$ suppressed, respectively. On the other hand, we have (see Eq. (5.9))

$$B = 3/4 + 0(1/N) \tag{6.10}$$

such that the uncertainties listed above simply disappear. Last but not least, a clean long--short distance separation is feasible in this limit. We can indeed divide the integration over the q^2-momentum of the virtual W-gauge bosons into two parts [52]. Below the cut-off $\Lambda = 0(1\ \text{GeV})$, we use the non-linear σ-model truncated to the pseudoscalars (Fig. 26a, b) with $m_K^2 \ll \Lambda^2$. Above this cut-off, we estimate the standard quark box-diagram contribution to the $K_L - K_S$ mass difference (Fig. 26c) with $m_K^2 \gg \Lambda^2$. We emphasize the identity of the meson and quark loop-momenta. This simple complementary approach has been successfully applied to the electromagnetic $\pi^+ - \pi^0$ mass difference in Section 3.

A straightforward one-loop calculation gives then

$$M^2 = m_c^2 - \Lambda^2 + m_K^2 \ln \frac{m_c^2}{\Lambda^2} - \tfrac{5}{6} m_K^2$$

$$+ \tfrac{7}{4} \Lambda^2 - \tfrac{3}{4} m_K^2 \ln \frac{\Lambda^2}{m_K^2} + \tfrac{11}{24} m_K^2 \tag{6.11}$$

for the quark and meson contributions, respectively. We notice a remarkable stability of Δm with respect to variations of the cut-off Λ between the kaon and charm quark masses (see Fig. 27). A minimum occurs for $\Lambda = 0.76\ \text{GeV} \simeq m_\rho$, independently of the charm quark mass. For $m_c = (1.5 \pm 0.1)\ \text{GeV}$, we conclude that

$$\Delta m = (0.8 \pm 0.1) \Delta m^{\text{exp}} \tag{6.12}$$

in the large-N limit.

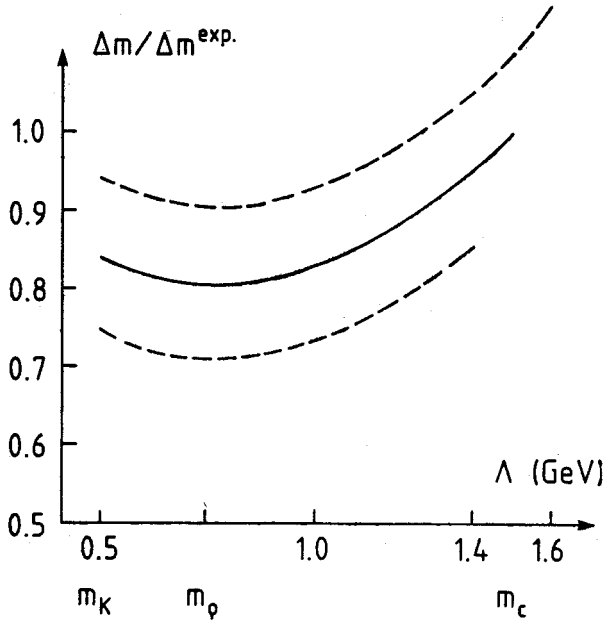

Fig. 27. The $K_L - K_S$ mass difference as a function of the W-gauge boson momentum cut-off, for $m_c = 1.5$ GeV (full line), 1.6 GeV (upper dashed-line) and 1.4 GeV (lower dashed line)

We notice that an estimate of M^2 with the W-propagators integrated out, would have given

$$M^2 = m_c^2 - \Lambda^2 + \tfrac{2}{3} m_K^2 \ln \frac{m_c^2}{\Lambda^2} - \tfrac{5}{9} m_K^2$$

$$+ \tfrac{3}{2} \Lambda^2 - \tfrac{3}{4} m_K^2 \ln \frac{\Lambda^2}{m_K^2} + \tfrac{3}{8} m_K^2 \qquad (6.13)$$

namely a 5% correction to Δm. This result provides therefore further confidence on the similar approximation used for the $\Delta I = \frac{1}{2}$ rule (Section 4) and the B-parameter (Section 5).

Up to now, we have neglected the short-distance top quark contributions to the box-diagram. Although the associated Kobayashi-Maskawa mixing angles are small, a heavy top quark could in principle give rise to sizeable corrections. Assuming $40\ \text{GeV} \leqslant m_t \leqslant 130$ GeV and imposing the experimental constraints arising from B-physics (oscillations, semi-leptonic decays), we obtain a *positive* contribution to the $K_L - K_S$ mass difference

$$0.05 \leqslant \Delta m(\text{tt, tc})/\Delta m^{\text{exp}} \leqslant 0.15. \qquad (6.14)$$

In conclusion, we have successfully estimated the $K_L - K_S$ mass difference in the large-N approximation. Our result supports the large-N prediction on the B-parameter (see Eq. (6.10)). Similar calculations based on the lattice and QCD sum rules non-perturbative approaches are now requested to settle this important question.

The knowledge of the B-parameter implies a better control on the unique CP-violating phase of the standard electroweak model. The prediction given in (5.15) allows indeed a rather precise determination of the unique Kobayashi-Maskawa CP-violating phase from the experimental value of ε_K. We are then in a position to make a prediction on the CP-violating quantity ε'.

7. *Penguins, $\Delta I = \frac{1}{2}$ rule and ε'/ε*

The so-called penguin diagrams given in Fig. (28) have been introduced [33] to explain the $\Delta I = \frac{1}{2}$ rule. The gluon coupling being vector-like, they can indeed induce the following $(V-A)(V+A)$ operator:

$$Q_p \equiv \sum_q \left\{ \bar{s}_i (\lambda_\alpha)^{ij} \gamma_\mu (1-\gamma_5) d_j \right\} \left\{ \bar{q}_k (\lambda_\alpha)^{kl} \gamma_\mu \left(\frac{1+\gamma_5}{2} \right) q_l \right\}, \tag{7.1}$$

with i, j, k, l, the color indices and $q = u, d, s$. The Fierz relations given in (A.3) imply

$$Q_p = -8(\bar{s}_L q_R)(\bar{q}_R d_L) \tag{7.2}$$

in the large-N limit. Consequently the density-density penguin operator Q_p vanishes [53] at the leading order in the chiral expansion (see Eq. (2.2)). The derivative term introduced in Eq. (2.23) turns out to be the unique contribution [54] to Q_p at the next-to-leading order

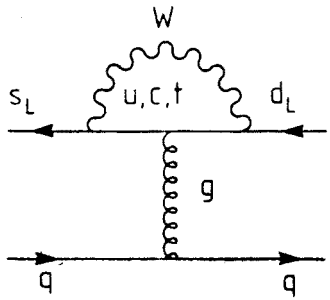

Fig. 28. The $\Delta S = 1$ penguin diagram

in the chiral expansion. Notice that "tadpole" operators $(mU^+)_{ds}$ induced by the non-derivative terms can be rotated away by a field redefinition. Consequently, they do not contribute to physical processes. We obtain then

$$\begin{aligned} Q_p &= -\frac{f^4 r^2}{8} \left\{ \left(U - \frac{1}{\Lambda_0^2} \partial^2 U \right) \left(U^+ - \frac{1}{\Lambda_0^2} \partial^2 U^+ \right) \right\}^{ds} \\ &= -\frac{f^4 r^2}{4\Lambda_0^2} (\partial_\mu U \partial_\mu U^+)^{ds} + O\left(\frac{1}{\Lambda_0^4} \right). \end{aligned} \tag{7.3}$$

The penguin operator Q_p is obviously a pure $\Delta I = \frac{1}{2}$ octet one (see Eq. (5.6)) and can be reexpressed in terms of the $Q_2^{\pi}(0)$ and $Q_1^{\pi}(0)$ operators defined in Eqs. (4.2) and (4.5) respectively. In the octet approximation, $\mathrm{Tr}(\partial_\mu U U^+) = 0$ such that

$$Q_p = \frac{r^2}{\Lambda_0^2}(Q_1 - Q_2)$$

$$\simeq 16(Q_1 - Q_2) \tag{7.4}$$

in the large-N limit (see Eqs. (2.3) and (2.27)). As we expected from a comparison with the short-distance evolution (4.9), the last operator in the "meson evolution" (4.6) is precisely the penguin one, which contributes constructively to the $\Delta I = \frac{1}{2}$ amplitudes. The enhancement factor $\frac{r^2}{\Lambda^2} \sim \frac{1}{4m_s^2}$ appearing in (7.4) partially compensates the typical $\frac{\alpha_s}{4\pi}$ suppression factor associated with the one-loop QCD-induced diagram of Fig. 28. Defining the ratio

$$R = \frac{A(\mathrm{K}^0 \to \pi^+\pi^-)}{A(\mathrm{K}^+ \to \pi^+\pi^0)} \tag{7.5}$$

we find [32] (for $\Lambda_{\mathrm{QCD}} = 0.3$ GeV):

$$R = \begin{cases} 13.0 & \text{if} \quad m_s = 125 \text{ MeV} \\ 11.7 & \quad\quad\; m_s = 150 \text{ MeV} \\ 10.9 & \quad\quad\; m_s = 175 \text{ MeV} \end{cases} \tag{7.6}$$

to be compared with the experimental value (see Eq. (4.4))

$$R^{\mathrm{exp}} \simeq 15. \tag{7.7}$$

The "weight" of the penguin diagram in the $\mathrm{K} \to \pi\pi$ $\Delta I = \frac{1}{2}$ enhancement can be inferred from the dependence on the strange quark mass defined at one GeV. It is worth stressing that the same $\frac{1}{N}$ approach applied to the $\pi^+ - \pi^0$ electromagnetic mass difference also favors a small value for $m_s(1\text{ GeV})$ (see Eq. (3.28)).

The penguin diagram with a virtual top quark (see Fig. 28) gives rise to a direct *CP*-violation in $\mathrm{K} \to \pi\pi$ decays, independently of the $\mathrm{K}^0 - \overline{\mathrm{K}}^0$ oscillations [55]. At the top quark mass scale, a short-distance calculation is reliable and we can express the *CP* violating parameter ε' in terms of the *B*-parameter and the strange quark mass arising from the $\Delta S = 2$ and $\Delta S = 1$ hadronic matrix elements respectively. As we have seen, these quantities can be estimated in the $\frac{1}{N}$ expansion approach for $\Lambda_{\mathrm{QCD}} = 0.3$ GeV. We obtain [56, 57]

$$\left(\frac{\varepsilon'}{\varepsilon}\right)_{\frac{1}{N}} = (2.5 \pm 1.5)\left\{\frac{0.7}{B}\right\}\left\{\frac{120 \text{ MeV}}{m_s(1\text{ GeV})}\right\}^2 10^{-3} \tag{7.8}$$

for 55 GeV $\lesssim m_t \lesssim$ 130 GeV and assuming [58] $0.01 \lesssim \bar{R} \equiv \Gamma(b \to u)/\Gamma(b \to c) \lesssim 0.06$. This result is consistent with the new measurement [39] of the NA31 Collaboration

$$\left(\frac{\varepsilon'}{\varepsilon}\right)^{\exp} = (3.3 \pm 1.1) 10^{-3}. \tag{7.9}$$

For illustration, the central experimental value is reproduced for $m_t = 70$ GeV and $\bar{R} = 1\%$. We stress that the prediction (7.8) has been *entirely* derived in a well-defined theoretical framework, the $\frac{1}{N}$ expansion approach, which provides us with — a satisfactory description of the $\Delta S = 1$ $K \to \pi\pi$ decay amplitudes ($\Delta I = \frac{1}{2}$ rule); — a consistent estimate of the $\Delta S = 2$ hadronic matrix element (B-parameter), and consequently, of the CP-violating Kobayashi-Maskawa phase.

In conclusion, we believe that the clash between the large $\Delta I = \frac{1}{2}$ octet enhancement and the small value of ε'/ε is only apparent and cannot be used to advocate new physics beyond the standard model. The $1/N$ expansion approach indicates that physics below one GeV is indeed quite important for the real part of $K \to \pi\pi$ decay amplitudes but negligible for their imaginary part.

8. Remarks and conclusion

Strong interaction quantum corrections to hadronic matrix elements are usually estimated within the $SU(N)_{QCD}$ quark-gluon theory. Asymptotic freedom allows a perturbative treatment of an amplitude as long as the loop-momentum is large compared to the typical one GeV confining scale. In these lectures, we have emphasized the importance of physics below one GeV for light meson processes. A large fraction of the $\pi^+ - \pi^0$ electromagnetic mass difference, of the $K \to \pi\pi$ weak decay amplitudes and of the $K_L - K_S$ mass difference arise from long-distance effects which can be estimated in a meson theory truncated to the low-lying bound states. Using the virtual photon (W-gauge boson) as a cheap probe, we find hints of the expected duality between a full meson theory and QCD in electromagnetic (weak) hadronic matrix elements, once the vector meson loop effects are taken into account. Eventually, both the theory with an infinite number of mesons (and glue-balls) and QCD should give the same strong interaction physics and, in particular, identical infrared and ultraviolet behaviours. It is therefore legitimate to ask if the well-known ultraviolet behaviour of QCD, namely asymptotic freedom, is already emerging from the meson theory truncated to the pseudoscalars and vectors.

In the chiral model defined in (3.15), the tree-level decay constant of the pion f_π is modified by one-loop meson corrections (see Fig. 29):

$$f_\pi = fX(M^2), \tag{8.1}$$

with

$$X(M^2) = 1 + n\left[-1 + \tfrac{9}{16}\, a\right] \frac{M^2}{(4\pi f)^2} - \tfrac{9}{16}\, na\, \frac{m_V^2}{(4\pi f)^2} \ln\left(1 + \frac{M^2}{m_V^2}\right). \tag{8.2}$$

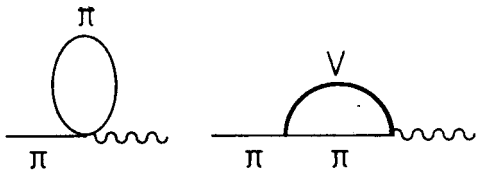

Fig. 29. Pseudoscalar and vector meson next-to-leading corrections o the decay constant f_π

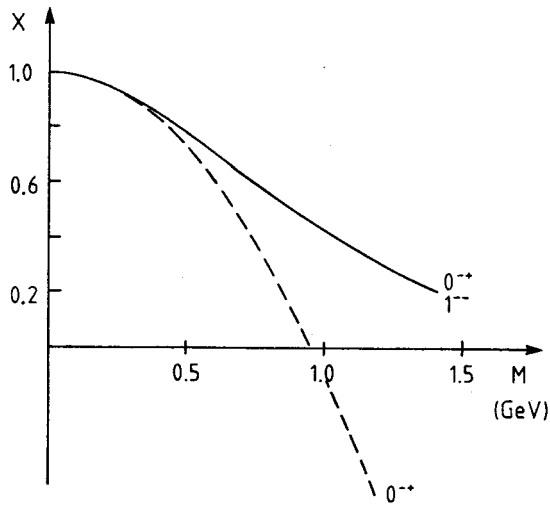

Fig. 30. Scale-dependence of the pseudoscalar mesons (dashed curve) and of the pseudoscalar plus vector mesons (full curve) one-loop corrections to the decay constant f_π

For $m_V^2 \gg M^2$ and $n = 3$, we recover the relation $f_\pi = f\left[1 - 3\frac{M^2}{(4\pi f)^2}\right]$ derived [32] in the meson theory truncated to the pseudoscalars. The function X is represented in Fig. 30 for the case of three flavors ($n = 3$) and $a = 2$.

On the other hand, the short-distance QCD corrections above the cut-off M must induce a momentum-dependence in f to keep the physical decay constant f_π scale-independent. In the $\frac{1}{N}$ expansion approach, the usual short and long-distance expansion parameters for strong interactions are respectively (see Eqs. (1.11) and (2.5))

$$\alpha_s \sim \frac{1}{N}, \quad (4\pi f)^{-2} \sim \frac{1}{N} \tag{8.3}$$

such that one expects

$$f(M^2) \sim \{\alpha_s(M^2)\}^{-1/2} \tag{8.4}$$

around one GeV. Consequently, the decrease of $X(M^2)$ for increasing values of the cut-off observed in Fig. 30 can be interpreted as a precocious asymptotic freedom behaviour. This nicely illustrates the role of the vector mesons in the matching with perturbative QCD.

In conclusion, the complementary approach based on the non-perturbative $\frac{1}{N}$ expansion enables us to analyse consistently the important interplay between electroweak and strong interactions around one GeV. We feel that this simple analytical method can give rather useful informations about new physics. In particular, we have seen that the $\Delta I = \frac{1}{2}$ rule, the $K_L - K_S$ mass difference and the *CP*-violating ε'/ε parameter do not seem to require physics beyond the standard model. *Physics below one GeV tells us something about physics above one TeV.* For example, the $K_L - K_S$ mass difference has been extensively used to constrain physics beyond the standard model. From the large-N approach presented here, we conclude that

$$|\Delta m \text{ (new physics)}| \leqslant 0.1\ \Delta m^{\text{exp}}. \tag{8.5}$$

Consequently, stronger constraints on hypothetical particles are allowed. For instance, the lower limit on the right-handed W gauge boson [59] reads now

$$M_{W_R} \geqslant 5 \text{ TeV} \tag{8.6}$$

in the (pseudo-) manifest left-right symmetric extension of the electroweak model.

I thank Bill Bardeen, Hans Bijnens, Andrzej Buras, Svjetlana Fajfer and Reinhold Rückl for enjoyable collaborations. Thanks are due to J. Donoghue, B. Guberina, L. Maiani, P. Minkowski, R. Peccei, T. Pich, E. de Rafael, B. and F. Schrempp and M. Shifman for very useful discussions.

APPENDIX A

Short-distance $\pi^+ - \pi^0$ mass difference

Let us estimate the one-loop contributions associated with the Feynman diagrams of Figs. (13a) and (13b) in the chiral limit ($m_u = m_d = 0$). Using the relations

$$\begin{aligned}(\gamma^\mu\gamma^\nu\gamma^\varrho)(\gamma_\varrho\gamma_\nu\gamma_\mu) &= 10(\gamma^\alpha)(\gamma_\alpha) - 6(\gamma^\alpha\gamma_5)(\gamma_\alpha\gamma^5),\\ (\gamma^\mu\gamma^\nu\gamma^\varrho)(\gamma_\mu\gamma_\nu\gamma_\varrho) &= 10(\gamma^\alpha)(\gamma_\alpha) + 6(\gamma^\alpha\gamma_5)(\gamma_\alpha\gamma^5)\end{aligned} \tag{A1}$$

we find respectively:

$$\begin{aligned}I_{ab} = \int \frac{dq^2}{q^4} \Big\{ &\mp(2\xi - 5)\left[\bar{q}\gamma_\alpha \frac{\lambda^a}{2} Qq\right]\left[\bar{q}\gamma^\alpha \frac{\lambda^a}{2} Qq\right]\\ &-3\left[\bar{q}\gamma_\alpha\gamma_5 \frac{\lambda^a}{2} Qq\right]\left[\bar{q}\gamma^\alpha\gamma_5 \frac{\lambda^a}{2} Qq\right]\Big\} \cdot \alpha_{\text{QED}}\alpha_{\text{QCD}}\end{aligned} \tag{A2}$$

such that $I_a + I_b$ is gauge-independent. From the "Fierz" relations

$$(\lambda_a)^{ij}(\lambda^a)^{kl} = 2\left(\delta^{il}\delta^{kj} - \frac{1}{N}\delta^{ij}\delta^{kl}\right)[\bar{q}_1\gamma_\alpha(1-\gamma_5)q_2]\,[\bar{q}_3\gamma^\alpha(1-\gamma_5)q_4]$$

$$= [\bar{q}_1\gamma_\alpha(1-\gamma_5)q_4]\,[\bar{q}_3\gamma^\alpha(1-\gamma_5)q_2]\,[\bar{q}_1\gamma_\alpha(1-\gamma_5)q_2]\,[\bar{q}_3\gamma^\alpha(1+\gamma_5)q_4]$$
$$= -2[\bar{q}_1(1+\gamma_5)q_4]\,[\bar{q}_3(1-\gamma_5)q_2], \tag{A3}$$

with i, j, k, l the color indices, we obtain in the large-N limit

$$I_{a(b)} = -\tfrac{3}{2}\int \frac{dq^2}{q^4}\,[\bar{q}(1+\gamma_5)Qq]\,[\bar{q}(1-\gamma_5)Qq],$$
$$I_{b(a)} = -3\int \frac{dq^2}{q^4}\,[\bar{q}\gamma_\alpha(1-\gamma_5)Qq[\bar{q}\gamma^\alpha(1-\gamma_5)Qq] \tag{A4}$$

for $\xi = 1(4)$ respectively. In the chiral-limit ($m_u = 0$), the current-current operators sandwiched between two pions vanish so that we are left with density-density hadronic matrix elements. Consequently for $\xi = 1(4)$, only the first (second) diagram of Fig. 13 contributes to the mass splitting. The correspondence between the meson contributions (Fig. 12) and the quark-gluon contributions is therefore striking. From Eq. (2.2), we can express the density-density operator appearing in (A4) in terms of meson fields:

$$I_{b(a)} = -\tfrac{3}{32}\,\alpha_{\mathrm{QED}} f^4 \int \frac{dq^2}{q^4}\,(\alpha_{\mathrm{QCD}} r^2)\,\mathrm{Tr}\,(QUQU^+). \tag{A5}$$

The product $(\alpha_{\mathrm{QCD}} r^2)$ is almost scale-independent. In fact the renormalization group equation implies a weak $[\alpha_{\mathrm{QCD}}(q^2)/\alpha_{\mathrm{QCD}}(\mu^2)]^{1/9}$ dependence. Neglecting this dependence and expanding the meson operator in (A5), we finally obtain the result given in Eq. (3.3).

APPENDIX B

A simple derivation of Weinberg sum rules

Let us consider the following hadronic matrix elements for the axial and vector currents

$$\langle 0|J_\mu^A|\pi^+\rangle = +\frac{i}{2} f_\pi q_\mu,$$
$$\langle 0|J_\mu^A|a_1^+\rangle = -\tfrac{1}{2} f_A m_A \varepsilon_\mu,$$
$$\langle 0|J_\mu^V|\varrho^+\rangle = -\tfrac{1}{2} f_V m_V \varepsilon_\mu. \tag{B1}$$

If we saturate the vector-vector two-point function with the ϱ-exchange and the axial-axial one with the a_1 and π-exchanges, we find respectively [60]

$$4\langle J_\mu^V(q) J_\nu^V(-q)\rangle \sim \frac{(f_V m_V)^2}{q^2 - m_V^2}\left(-g_{\mu\nu} + \frac{q_\mu q_\nu}{m_V^2}\right) \tag{B2}$$

and

$$4\langle J_\mu^A(q) J_\nu^A(-q)\rangle \sim \frac{(f_A m_A)^2}{q^2 - {}^2}\left(-g_{\mu\nu} + \frac{q_\mu q_\nu}{m_A^2}\right) + \frac{f_\pi^2}{q^2}\, q_\mu q_\nu. \tag{B3}$$

In the case of an exact chiral $SU(2)_L \times SU(2)_R$ symmetry, Eqs. (B2) and (B3) are identical and we obtain $f_\pi = 0$, $m_A = m_V$, $f_A = f_V$. On the other hand, if the spontaneously broken $SU(2)_L \times SU(2)_R$ symmetry is restored only at very high momentum ($q^2 \to \infty$), we obtain the famous Weinberg sum rules

$$f_V^A = f_A^2 + f_\pi^2, \quad f_V m_V = f_A m_A \tag{B4}$$

by identifying the coefficients of $q_\mu q_\nu$ and $q_{\mu\nu}$ respectively. The relations (B4) together with the KSRF relation (3.21) lead to Eq. (3.25).

REFERENCES

[1] See e.g. P. Langacker, talk presented at the XXIV International Conference on High Energy Physics, Munich 1988.

[2] G.'t Hooft, in Recent Developments in Gauge Theories, Proceedings of the NATO Advanced Study Institute, Cargèse 1979, ed. G.'t Hooft et al., Plenum, New York 1980.

[3] See e.g. L. Hall, talk presented at the XXIV International Conference on High Energy Physics, Munich 1988.

[4] See e.g. the Proceedings of the Ringberg Workshop on Hadronic Matrix Elements and Weak Decays, April 1988, *Nucl. Phys.* **B** (Proc. Suppl.) **7A** (1989), Ed. A. J. Buras, J.-M. Gérard, W. Huber.

[5] G.'t Hooft, *Nucl. Phys.* **B72**, 461 (1974); *Nucl. Phys.* **B75**, 461 (1974).

[6] E. Witten, *Nucl. Phys.* **B160**, 57 (1979).

[7] See also, W. A. Bardeen, Contribution to the Ringberg Workshop 1988, Ref. [4]; A. J. Buras, Lectures given at the XIX International Seminar on Theoretical Physics, Jaca, Spain 1988.

[8] Y. Nambu, G. Jona-Lasinio, *Phys. Rev.* **D122**, 345 (1961).

[9] M. A. Shifman, A. I. Vainshtein, V. I. Zakharov, *Nucl. Phys.* **B147**, 385, 448, 519 (1979).

[10] J. Bardeen, L. N. Cooper, J. R. Schrieffer, *Phys. Rev.* **106**, 162, (1957); **108**, 1175 (1957).

[11] R. P. Feynman, Gauge theories, in Les Houches 1976 Proceedings on Weak and Electromagnetic Interactions at High Energies, Amsterdam 1977, pp. 121–206.

[12] S. Coleman, E. Witten, *Phys. Rev. Lett.* **45**, 100 (1980).

[13] C. Rosenzweig, J. Schechter, G. Trahern, *Phys. Rev.* **D21**, 3388 (1980); P. Di Vecchia, G. Veneziano, *Nucl. Phys.* **B171**, 253 (1980); E. Witten, *Ann. Phys.* **128**, 363 (1980).

[14] See e.g., K. R. Schubert, in Proceedings of the 1987 EPS Conference, Uppsala, 1987; E. A. Paschos in the Proceedings of the Ringberg Workshop, Ref. [4].

[15] H. Leutwyler, M. Roos, *Z. Phys.* **C25**, 91 (1984).

[16] For a nice introduction, see H. Georgi, Weak Interaction and Modern Particle Theory Benjamin/Cummings, Menlo Park 1984.

[17] D. G. Sutherland, *Phys. Lett.* **23**, 384 (1966).

[18] R. Dashen, *Phys. Rev.* **183**, 1245 (1969).

[19] S. Weinberg, *Trans. N. Y. Acad. Sci.* **38**, 185 (1977).

[20] S. Weinberg, *Phys. Rev.* **D11**, 3583 (1975).

[21] F. J. Gilman, R. Kauffman, *Phys. Rev.* **D36**, 2761 (1987).

[22] D. B. Kaplan, A. V. Manohar, *Phys. Rev. Lett.* **56**, 2004 (1986); see also, J. M. Cline, *Phys. Rev. Lett.* **63**, 1338 (1989).

[23] J.-M. Gérard, Max-Planck preprint MPI-PAE/PTh 62/89, 1989.

[24] J. Gasser, H. Leutwyler, *Phys. Rep.* **C87**, 77 (1982), and references therein.

[25] W. A. Bardeen, J. Bijnens, J.-M. Gérard, *Phys. Rev. Lett.* **62**, 1343 (1989).

[26] J. Gasser, H. Leutwyler, *Nucl. Phys.* **B250**, 465 (1985).

[27] See M. Bando, T. Kugo, K. Yamawaki, *Phys. Rep.* **C164**, 217 (1988); V. G. Meissner, *Phys. Rep.* **C161**, 213 (1988), and references therein.

[28] K. Kawarabayashi, M. Suzuki, *Phys. Rev. Lett.* **16**, 225 (1966); Riazuddin Fayyazuddin, *Phys. Rev.* **147**, 1071 (1966).
[29] S. Weinberg, *Phys. Rev. Lett.* **18**, 507 (1967).
[30] T. Dass et al., *Phys. Rev. Lett.* **18**, 759 (1967).
[31] R. D. Peccei, J. Solà, *Nucl. Phys.* **B281**, 1 (1987).
[32] W. A. Bardeen, A. J. Buras, J.-M. Gérard, *Phys. Lett.* **192B**, 138 (1987).
[33] A. I. Vainshtein, V. I. Zakharov, M. A. Shifman, *Sov. Phys. JETP* **45**, 670 (1977).
[34] M. K. Gaillard, B. W. Lee, *Phys. Rev. Lett.* **33**, 108 (1974); G. Altarelli, L. Maiani, *Phys. Lett.* **52B**, 351 (1974).
[35] A. J. Buras, J.-M. Gérard, R. Rückl, *Nucl. Phys.* **B268**, 16 (1986).
[36] M. Bauer, B. Stech, M. Wirbel, *Z. Phys.* **C34**, 103 (1987), and references therein.
[37] W. A. Bardeen, A. J. Buras, J.-M. Gérard, *Nucl. Phys.* **B293**, 787 (1987).
[38] For other attempts, see Ref. [4].
[39] NA31 Collaboration, H. Burkhardt et al., *Phys. Lett.* **206B**, 169 (1988).
[40] M. K. Gaillard, B. W. Lee, *Phys. Rev.* **D10**, 897 (1974).
[41] J. F. Donoghue, E. Golowich, B. R. Holstein, *Phys. Lett.* **119B**, 412 (1982).
[42] J. Bijnens, H. Sonoda, M. B. Wise, *Phys. Rev. Lett.* **53**, 2367 (1984).
[43] A. J. Buras, J.-M. Gérard, *Nucl. Phys.* **B264**, 371 (1986).
[44] W. A. Bardeen, A. J. Buras, J.-M. Gérard, *Phys. Lett.* **211B**, 343 (1988).
[45] J.-M. Gérard, talk presented at the XXIV International Conference on High Energy Physics, Munich 1988.
[46] See e.g. J.-M. Gérard, Max-Planck preprint MPI-PAE/PTh 32/89, to appear in the Proceedings of the International Workshop on Weak Interactions and Neutrinos Ginosar, Israel, April 1989.
[47] See e.g. R. N. Mohapatra, J. Subba Rao, R. E. Marshak, *Phys. Rev. Lett.* **20**, 1081 (1968); C. Bouchiat, J. Iliopoulos, J. Prentki, *Nuovo Cimento* **56A**, 1150 (1968).
[48] S. L. Glashow, J. Iliopoulos, L. Maiani, *Phys. Rev.* **D2**, 1285 (1970).
[49] L. Wolfenstein, *Nucl. Phys.* **B160**, 501 (1979).
[50] F. J. Gilman, M. B. Wise, *Phys. Rev.* **D27**, 1128 (1983).
[51] A. Datta, D. Kumbhakar, *Phys. Rev.* **D33**, 3461 (1986). Notice that the authors have used the vacuum insertion approximation to estimate the hadronic matrix elements. Here we present the results in the large-N limit
[52] J.-M. Gérard, Max Planck preprint MPI-PAE/PTh 41/89, to appear in the Proceedings of the 12th Warsaw Symposium on Elementary Particle Physics, Kazimierz, May 1989; J. Bijnens, J.-M. Gérard, G. Klein, in preparation.
[53] Y. Dupond, T. N. Pham, *Phys. Rev.* **D29**, 1368 (1984).
[54] R. S. Chivukula, J. M. Flynn, H. Georgi, *Phys. Lett.* **171B**, 453 (1986); W. A. Bardeen, A. J. Buras, J.-M. Gérard, *Phys. Lett.* **180B**, 133 (1986).
[55] F. J. Gilman, M. B. Wise, *Phys. Lett.* **83B**, 83 (1979).
[56] J.-M. Gérard, Proceedings of the VIIth Moriond Workshop on New and Exotic Phenomena, 1987, p. 89.
[57] A. J. Buras, J.-M. Gérard, *Phys. Lett.* **203B**, 272 (1988).
[58] See e.g. K. Kleinknecht, talk presented at the XXIV International Conference on High Energy Physics, Munich 1988.
[59] G. Beall, M. Bander, A. Soni, *Phys. Rev. Lett.* **48**, 848 (1982).
[60] J. J. Sakurai, *Currents and Mesons*, The University of Chicago Press.